SKB

TECHNICAL REPORT 87-03

Calculations on HYDROCOIN level 1 using the GWHRT flow model

Case 1 Translent flow of water from a borehole penetrating a confined aquifer

Case 3 Saturated-unsaturated flow through a layered sequence of sedimentary rocks

Case 4 Translent thermal convection in a saturated medium

Roger Thunvik, Royal Institute of Technology, Stockholm

March 1987

SVENSK KÄRNBRÄNSLEHANTERING AB
SWEDISH NUCLEAR FUEL AND WASTE MANAGEMENT CO
BOX 5864 S-102 48 STOCKHOLM
TEL 08-665 28 00 TELEX 13108-SKB

CALCULATIONS ON HYDROCOIN LEVEL 1 USING THE GWHRT FLOW MODEL

Case 1 Transient flow of water from a borehole penetrating a confined aquifer

Case 3 Saturated-unsaturated flow through a layered sequence of sedimentary rocks

Case 4 Transient thermal convection in a saturated medium

Roger Thunvik
Royal Institute of Technology, Stockholm

March 1987

Abstract

The present report presents solutions to Hydrocoin Level 1: Case 1, 3 and 4. Case 1 deals with transient flow of water from a borehole which penetrates a confined aquifer consisting of a homogeneous, isotropic permeable medium which is underlain by a single horizontal fracture. Case 3 deals with a problem of saturated-unsaturated flow through a layered sequence of sedimentary rocks. Case 4 deals with transient thermal convection in a saturated permeable medium.

Hydrocoin is an international cooperation project to compare different computer models used for describing groundwater flow in geological media. The purpose of the project is to improve the understanding of various strategies for modelling groundwater flow for the safety assessment of final radioactive waste repositories.

The project is structured in three levels. The object of level 1 is to examine the numerical accuracy of the computer models compared. The object of level 2 is to study the capability of computer models to describe in-situ measurements. Level 3 is concerned with sensitivity and uncertainty analysis of groundwater flow.

SUMMARY

The present report presents solutions to Hydrocoin Level 1: Case 1, 3 and 4. Case 1 deals with transient flow of water from a borehole which penetrates a confined aquifer consisting of a homogeneous, isotropic permeable medium which is underlain by a single horizontal fracture. Case 3 deals with a problem of saturated-unsaturated flow through a layered sequence of sedimentary rocks. Case 4 deals with transient thermal convection in a saturated permeable medium.

The calculations were carried out using the GWHRT-flow model for calculation of coupled flow of groundwater and heat in fractured rock. The model is used for the calculation of groundwater flow at study sites included in the Swedish research program (Swedish Nuclear Fuel Co) for studying the final storage of radioactive waste in hard rock repositories.

The GWHRT-model solves for one, two or three-dimensional saturated-unsaturated flow of water and heat through a fractured rock mass, treated either as a single equivalent continuum or as two overlapping continua. Fluid density is assumed to be dependent of pressure and temperature, while the dynamic viscosity of the fluid is assumed to be dependent of temperature only.

Hydrocoin is an international cooperation project to compare different computer models used for describing groundwater flow in geological media. The purpose of the project is to improve the understanding of various strategies for modelling groundwater flow for the safety assessment of final radioactive waste repositories.

The project is structured in three levels. The object of level 1 is to examine the numerical accuracy of the computer models compared. The object of level 2 is to study the capability of computer models to describe in-situ measurements. Level 3 is concerned with sensitivity and uncertainty analysis of groundwater flow.

Case 1

The purpose of this case was to simulate an ideal test problem dealing with transient saturated flow from a borehole in a permeable medium underlain by a single horizontal fracture. Initially the head in both the rock matrix and the fracture was zero. A time-dependent head was prescribed in the borehole. The object was to calculate the head in the rock matrix and to present time-dependent solutions for the head at two points and to present the head profile at a given depth and point of time according to the specification document.

The rock matrix is characterized by a hydraulic conductivity and a specific storage. The fracture is characterized by a transmissivity and a storage coefficient. In the calculations a finite width was attributed to the fracture, which was represented by two-dimensional elements.

The horizontal extent of the flow domain is 10 metres and the vertical extent is 5 metres, respectively. Porosity was assumed to be 0.1 and the fracture was attributed a width of 0.01 m. The parameter data given in the specification document were transformed into units suitable for the flow model equation as follows.

The element mesh was successively densified until good agreement between the numerical and the analytical solution values could be obtained. The final solution was worked out using a mesh of 195 8-node quadri-lateral elements and 642 nodes. Time was advanced in logarithmically distributed time steps for about 100 time steps.

Case 3

The purpose of this case was to simulate the flow through a layered sequence of sedimentary rocks. The flow domain is characterized by a strong vertical variation of the flow conditions. The horizontal extent of the flow domain is 2000 metres and the maximum vertical depth of the flow domain is 1500 metres.

Unsaturated flow occurs in the upper part of the flow domain. A constant infiltration rate is prescribed on the top boundary of the flow domain. The lateral boundary is characterized by a seepage face and a hydrostatic boundary representing a lake *)

The object of the present computational exercise was to simulate the transient drawdown and the steady state position of the water table, which initially was assumed to be located at the top surface. The physical properties at unsaturated conditions such as the capillary pressure and the relative permeability versus saturation were prescribed in the specification document of the case.

A set of preliminary calculations exhibited serious convergence problems using the prescribed original parameter data. Obviously, the numerical problems were due to the extremely high permeability contrasts which occurred when the water table penetrated the aquitard located in the flow domain. It was concluded that solving the flow problem using the original data would require development beyond the considered purpose of the flow model used in the calculations. Therefore, it was decided to seek some solutions for simplified flow conditions in order to study the applicability of the flow model used.

---

*) The characteristics of the flow domain considered in this case originates from a study site for radioactive waste in Switzerland.

The solutions were worked out using the original data until the solution was destroyed. This usually occured within one or two time steps after the water table had reached the aquitard. Thereafter restarts were made using the simplified parameter data. Usually, the solutions could be advanced 10-15 time steps without much problem to a situation with the water table located at about 375 metres on the left hand side.

In a first attempt to achieve a steady state solution to the problem the relative permeability was set constant and equal to one for all saturations. The simulation was resumed just before the solution with the original data failed, i.e. with the water table located at about 375 metres on the left hand side. As a result the solution could readily be advanced to steady state and the water table reached a position of the water table at about 65 metres on the left hand side.

In a second attempt to reach steady state the minimum value of the relative permeability was set equal to 0.25 when the water table on the left hand side was located at 375 metres. The solution could now be advanced fairly easy to a steady state position with the water table at a level of about 220 metres on the left hand boundary. The water table is thus entirely located below the aquitard. Some oscillatory behaviour of the water table could be observed at the left hand boundary, but the final flow conditions appeared to be quite stable.

In a third attempt to reach steady state the conditions were the same as for in the second attempt, but the solution was advanced using much smaller time steps in order to avoid the oscillatory behaviour on the left hand boundary. In this case steady state conditions were achieved with the water table located above the aquitard on the left hand boundary. It is not yet clear, however, whether the contradictions in the solutions obtained here are realistic or simply the result of improper numerical treatment of the problem.

Generally, it may be concluded from the previous calculations that the problem exactly as defined in the specification document could not be solved with the present version of the computer model used in the calculations. Furthermore, it may be concluded that simplifying assumptions such as those made in the calculations may

change the behaviour of the flow problem and lead to erroneous solutions.

Among the features that should be developed or implemented in the present numerical model to facilitate the treatment of unsaturated flow could be mentioned time step control algorithms and mesh adaptive techniques.

Case 4

This case deals with transient thermal convection in a saturated permeable medium. An analytical solution was also presented and the numerical results worked out in the present study are presented together with the analytical solution. The purpose of this case is to calculate time dependent buoyancy driven flows due to heat released from a hypothetical radioactive waste repository.

The problem is characterized by a low Rayleigh number and it is assumed that the heat flow is mainly due to conduction. The repository is represented by a spherical exponentially decaying heat source. The surrounding rock mass is assumed to be homogeneous and isotropic. The same material properties are assumed for the repository as for the surrounding rock mass.

Very good agreement between the results from the numerical and the analytical model could be obtained for the main predicted variables in the flow model, viz. pressure and temperature. Numerical problems were encountered when predicting the long term pathlines. It is believed that the pathline tracking problems were mainly due to the exceedingly large time steps that were used towards the end of the simulation period. In the present time step selection scheme no consideration is made with regard to the pathline tracking.

A further numerical problem associated with the pathline tracking are are even further aggravated by the fact that the present element type and evaluation of the velocities may lead to intrinsic inconsistencies in the velocity field, especially in regions where the density gradients are relatively small.

HYDROCOIN Level 1, Case 1
Transient flow of water from a borehole penetrating a confined aquifer

Roger Thunvik
Rina Rotshild

Royal Institute of Technology
Stockholm, Sweden

Contents

Introduction

The purpose of the present study is to simulate and ideal test problem dealing with transient saturated flow from a borehole in a permeable medium, which is underlain by a single horizontal fracture. The problem together with an analytical solution was specified by Hodgkinson and Barker (1). The flow domain considered is illustrated in Figure 1. The numerical results carried out in the present report are displayed graphically together with the analytical ones.

Flow model

The flow model used in the calculations was developed by Thunvik and Braester (2). It is assumed that the flow in the rock matrix as well as in the fracture can be described by Darcy's law. From Darcy's law and the equation for the conservation of mass the following equation is used in the calculations

$$\phi\rho^f(c^f + c^r)\, p_{,t} - (\rho^f \frac{k}{\mu}_{ij}\, (p_{,j} - \rho^f g_j) + Q = 0$$

where ϕ is porosity, c^f is fluid compressibility, c^r is rock compressibility, p is pressure, t is time, k_{ij} is the permeability tensor, ρ^f is fluid density, μ is the dynamic viscosity, g is the acceleration of gravity and Q represents a mass source.

The flow equation is solved numerically using the Galerkin finite element method. The algebraic system of equations resulting from the Gauss integration over the elements is solved by Gauss elimination using the frontal method.

Boundary conditions

Initially the head in both the rock matrix and the fracture is zero. The following time-dependent head is prescribed in the borehole (see Figure 1)

$$h_a(t) = h\,(1 - \exp(-t/\tau))$$

where τ is a time constant. No-flow boundary conditions are assumed on the top and bottom boundaries respectively and prescribed zero head is prescribed at the lateral boundary.

Input parameters

The rock matrix is characterized by a hydraulic conductivity (K) and a specific storage (S_s). The fracture is characterized by a transmissivity (T) and a storage coefficient (S). In the calculations a finite width is attributed to the fracture, which was represented by two-dimensional elements. Porosity was assumed to be 0.1 and the fracture was attributed a width of 0.01 m. The parameter data given in the specification document are transformed into units suitable for the model equation as follows.

The specific storage is defined as

$$S_s = \phi \rho g c$$

where ϕ is porosity, ρ is the fluid density, g is the acceleration of gravity and c is the total compressibility of the rock matrix, which then becomes

$$c = 10^{-7}/(0.1*10^{3}*9.81) = 1.0193679*10^{-10}\ Pa^{-1}$$

The storage coefficient is defined as

$$S = \phi \rho g c b$$

where b is the fracture width. The compressibility in the fracture then becomes

$$c = 10^{-10}/(0.1*10^{3}*9.81*0.01) = 1.0193679*10^{-11}\ Pa^{-1}$$

Hydraulic conductivity and transmissivity are defined as

$$K = k \frac{\rho g}{\mu} \quad , \quad T = kb$$

Using these relationships then the rock permeability becomes

$$k = 10^{-9} \frac{10^{-3}}{9.81*10^{3}} = \frac{1}{9.81} * 10^{-15} = 1.0193679*10^{-16}\ m^2$$

The fracture permeability becomes

$$k = 10^{-8} \frac{10^{-3}}{9.81*10^{3}*10^{-2}} = \frac{1}{9.81} *10^{-12} = 1.0193679*10^{-13}\ m^2$$

Table of input data

Symbol	Parameter	Value	Unit
ρ	Density	10^3	kgm^{-3}
μ	Dynamic viscosity	10^{-3}	Pas
ϕ	Porosity	0.1	-
a	Radius of borehole	0.1	m
b	Radial distance to boundary	10	m
τ	Time constant for borehole head	0.1	s
fracture			
k	Permeability	$1.01936*10^{-13}$	m^2
d	Width	0.01	m
c	Compressibility	$1.01936*10^{-11}$	Pa^{-1}
rock matrix			
k	Permeability	$1.01936*10^{-16}$	m^2
d	Thickness	5.0	m
c	Compressibility	$1.01936*10^{-10}$	Pa^{-1}

Results

The element mesh was successively densified until it could be observed on graphical displays of the results that there was good agreement between the numerical and the analytical solution values. The final solution was worked out using a mesh of 195 8-node quadri-lateral elements and 642 nodes. The mesh used is shown in Figures 4 and 5. Time was advanced in logarithmically distributed time steps for about 100 time steps. The numerical results were found to be in very good agreement with the analytical solution. The results of the calculations are shown in Figures 2-4 and Tables 1-3 in the Appendix.

References

1. Hodgkinson,D. and Barker, J., 1985, Specification of a test problem for HYDROCOIN Level 1 Case 1: Transient flow from a borehole in a fractured permeable medium, AERE - R 11574, HARWELL.

2. Thunvik,R. and Braester, C., 1980, Hydrothermal conditions around a radioactive waste repository, Part 1 - A mathematical model for the flow of groundwater and heat in fracture rock, part 2 - Numerical solutions, Part 3 - Numerical solutions for anisotropy, SKBF-KBS-TR:80-19.

List of figures

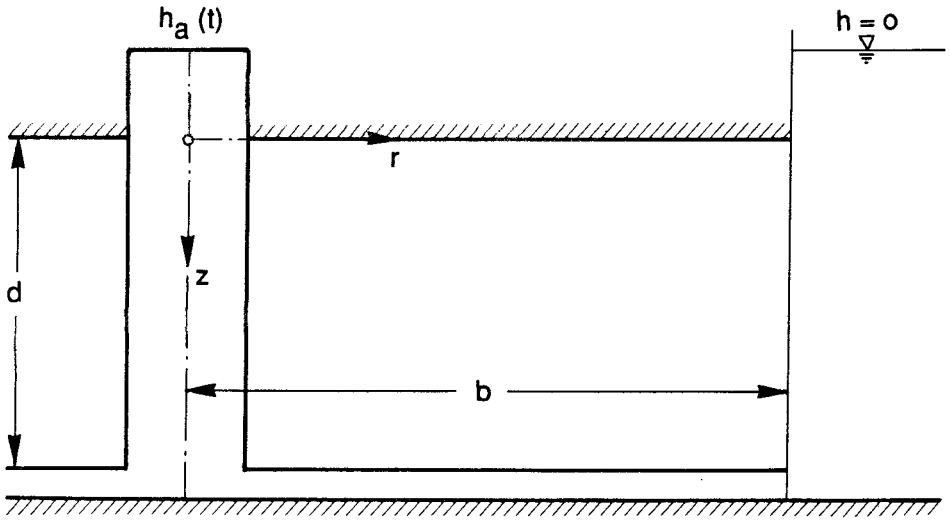

Figure 1.

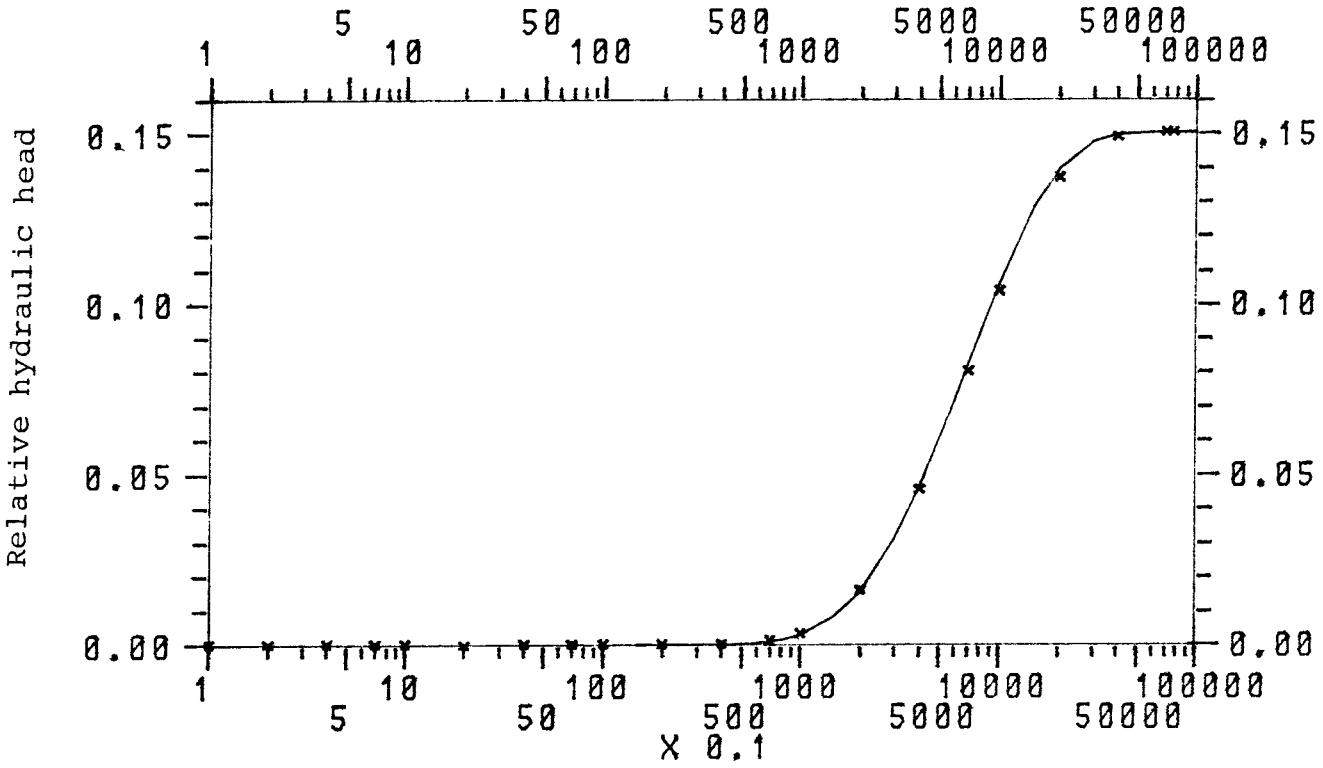

Figure 2.

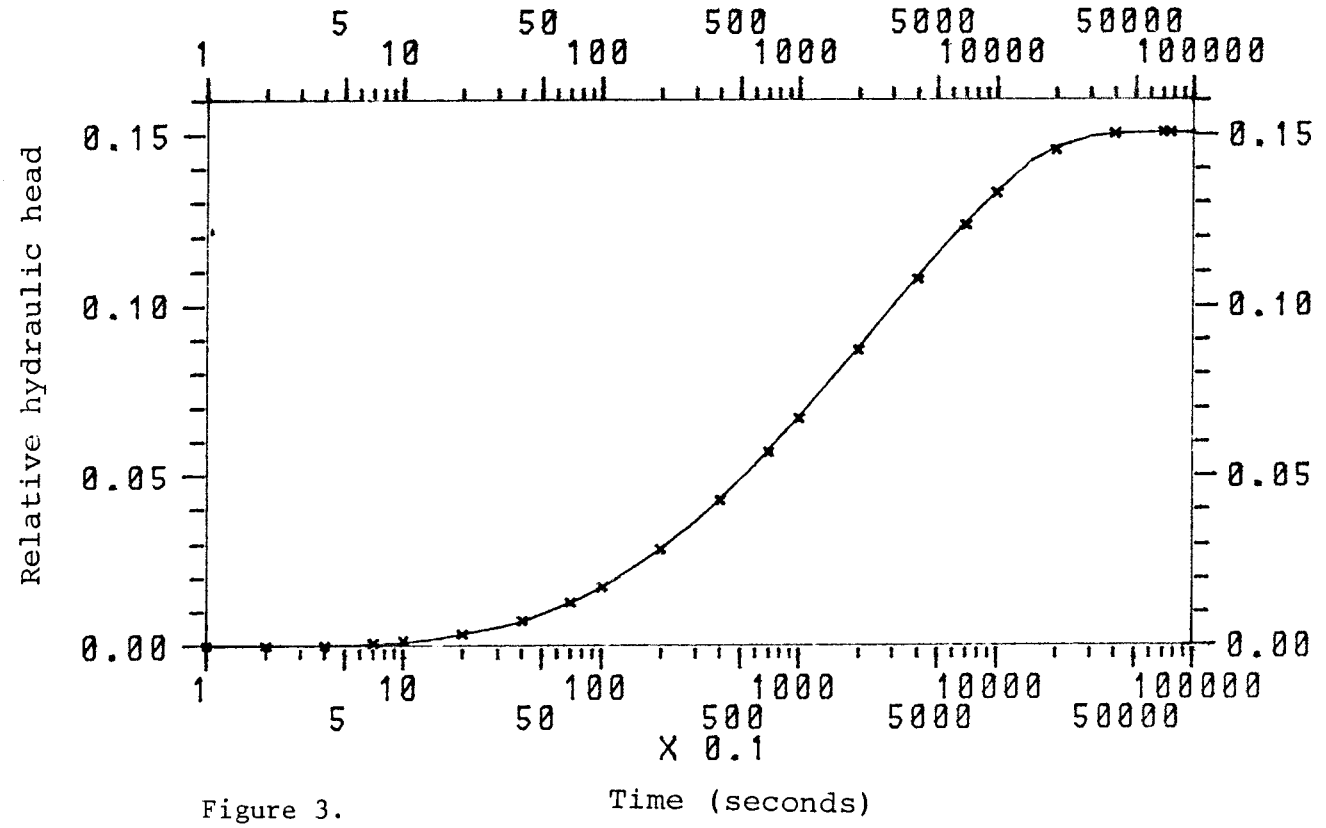

Figure 3.

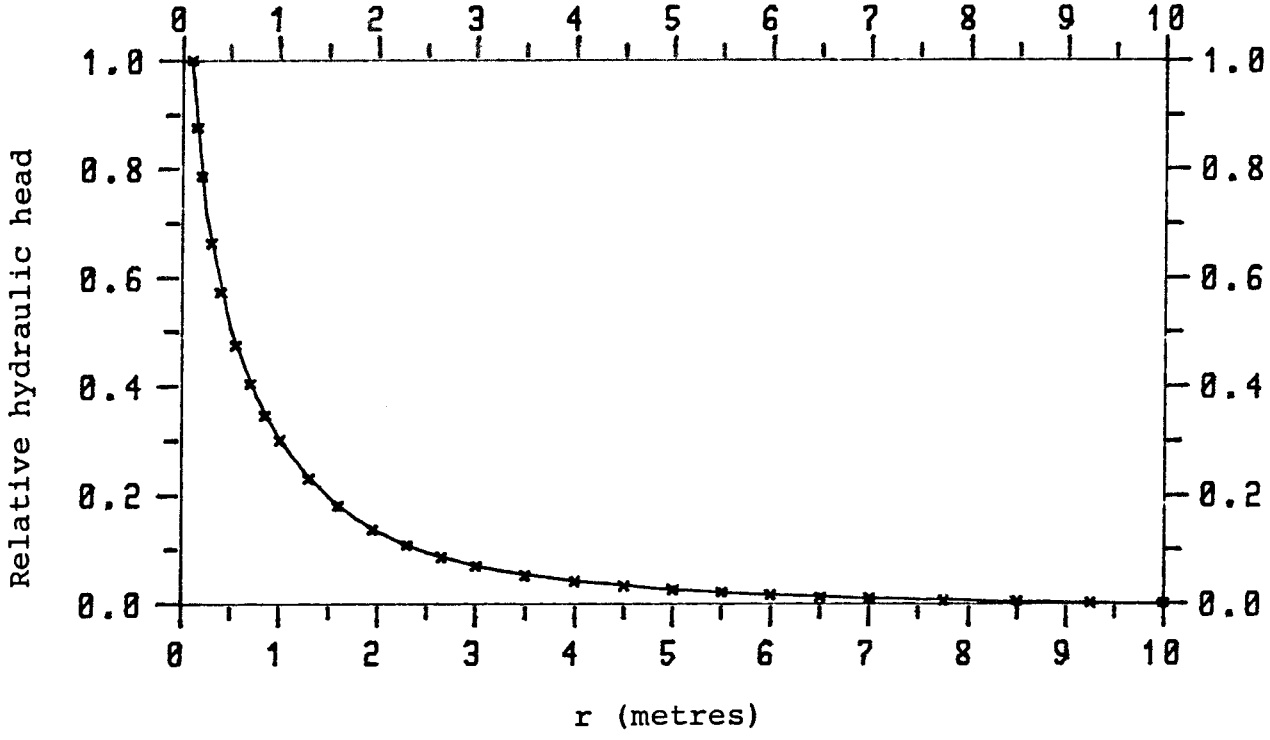
Relative hydraulic head
0 1 2 3 4 5 6 7 8 9 10
1.0
0.8
0.6
0.4
0.2
0.0
r (metres)

Figure 4.

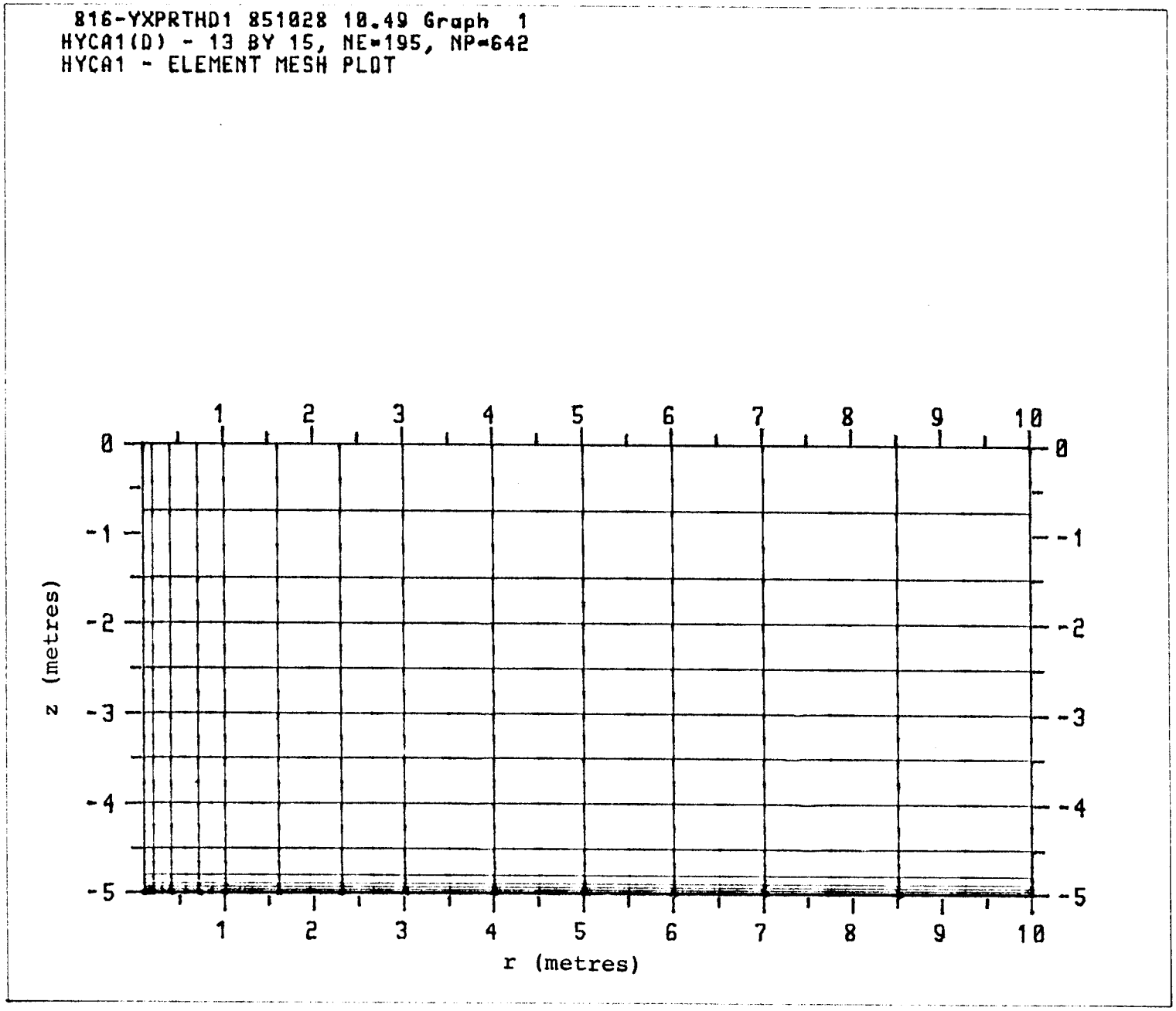
816-YXPRTHD1 851028 10.49 Graph 1
HYCA1(D) - 13 BY 15, NE=195, NP=642
HYCA1 - ELEMENT MESH PLOT
1 2 3 4 5 6 7 8 9 10
0
-1
-2
-3
-4
-5
z (metres)
r (metres)

Figure 5.

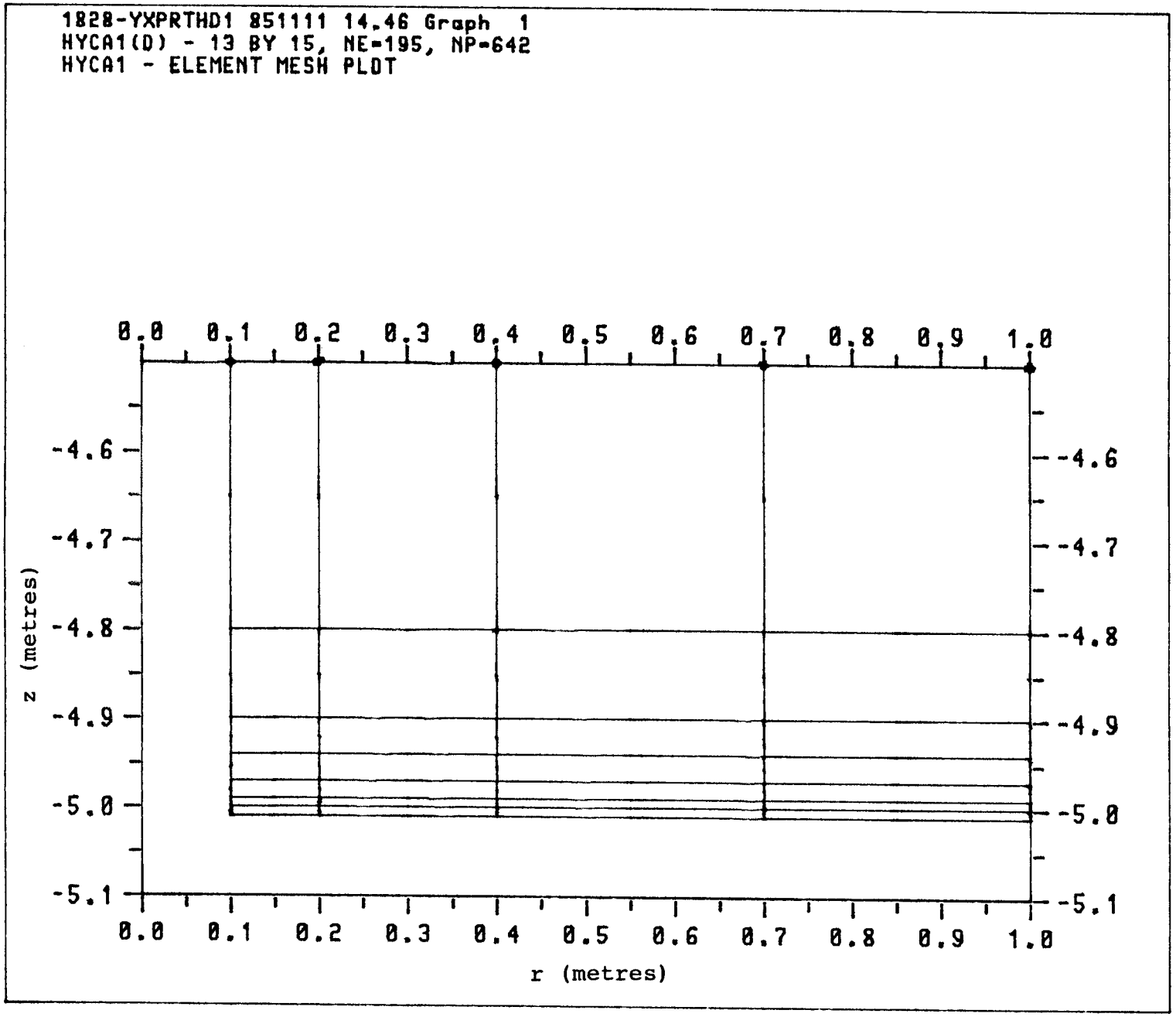
1828-YXPRTHD1 851111 14.46 Graph 1
HYCA1(D) - 13 BY 15, NE=195, NP=642
HYCA1 - ELEMENT MESH PLOT
0.0
0.1
0.2
0.3
0.4
0.5
0.6
0.7
0.8
0.9
1.0
-4.6
-4.7
-4.8
-4.9
-5.0
-5.1
z (metres)
r (metres)

Figure 6.

Appendix: Tables of results submitted to the project secreteriat

Table 1. Numerical solution for the time dependent relative hydraulic head at r=5 m and z=2.5 m.

Table 2. Numerical solution for the time dependent relative hydraulic head at r=5 m and z=5.0 m.

Table 3. Numerical solution for the relative hydraulic head versus distance at z=4 m and t=100 s.

Table 1

1 HDRL1C1N: Table 1 - Numerical Solution, R=5m, Z=2.5m
21 Number of lines to follow

5.00000E+00	-2.50000E+00	1.00000E-01	7.82099E-11
5.00000E+00	-2.50000E+00	2.00000E-01	5.67312E-10
5.00000E+00	-2.50000E+00	4.00000E-01	-2.69474E-10
5.00000E+00	-2.50000E+00	7.00000E-01	1.11385E-10
5.00000E+00	-2.50000E+00	1.00000E+00	-1.04301E-09
5.00000E+00	-2.50000E+00	2.00000E+00	-8.78910E-09
5.00000E+00	-2.50000E+00	4.00000E+00	1.00970E-08
5.00000E+00	-2.50000E+00	7.00000E+00	3.32533E-08
5.00000E+00	-2.50000E+00	1.00000E+01	3.33194E-08
5.00000E+00	-2.50000E+00	2.00000E+01	2.17085E-06
5.00000E+00	-2.50000E+00	4.00000E+01	1.18094E-04
5.00000E+00	-2.50000E+00	7.00000E+01	1.08800E-03
5.00000E+00	-2.50000E+00	1.00000E+02	3.18535E-03
5.00000E+00	-2.50000E+00	2.00000E+02	1.58599E-02
5.00000E+00	-2.50000E+00	4.00000E+02	4.56031E-02
5.00000E+00	-2.50000E+00	7.00000E+02	8.03427E-02
5.00000E+00	-2.50000E+00	1.00000E+03	1.03819E-01
5.00000E+00	-2.50000E+00	2.00000E+03	1.37160E-01
5.00000E+00	-2.50000E+00	4.00000E+03	1.49168E-01
5.00000E+00	-2.50000E+00	7.00000E+03	1.50521E-01
5.00000E+00	-2.50000E+00	7.60000E+03	1.50551E-01

Table 2

2 HDRL1C1N: Table 2 - Numerical Solution, R=5m, Z=5.0m

21 Number of lines to follow

5.00000E+00	-5.00000E+00	1.00000E-01	4.90564E-06
5.00000E+00	-5.00000E+00	2.00000E-01	3.39282E-05
5.00000E+00	-5.00000E+00	4.00000E-01	2.02450E-04
5.00000E+00	-5.00000E+00	7.00000E-01	6.52311E-04
5.00000E+00	-5.00000E+00	1.00000E+00	1.22039E-03
5.00000E+00	-5.00000E+00	2.00000E+00	3.35000E-03
5.00000E+00	-5.00000E+00	4.00000E+00	7.44226E-03
5.00000E+00	-5.00000E+00	7.00000E+00	1.26974E-02
5.00000E+00	-5.00000E+00	1.00000E+01	1.71345E-02
5.00000E+00	-5.00000E+00	2.00000E+01	2.81996E-02
5.00000E+00	-5.00000E+00	4.00000E+01	4.26957E-02
5.00000E+00	-5.00000E+00	7.00000E+01	5.67382E-02
5.00000E+00	-5.00000E+00	1.00000E+02	6.66427E-02
5.00000E+00	-5.00000E+00	2.00000E+02	8.67254E-02
5.00000E+00	-5.00000E+00	4.00000E+02	1.07373E-01
5.00000E+00	-5.00000E+00	7.00000E+02	1.23383E-01
5.00000E+00	-5.00000E+00	1.00000E+03	1.32767E-01
5.00000E+00	-5.00000E+00	2.00000E+03	1.45502E-01
5.00000E+00	-5.00000E+00	4.00000E+03	1.50049E-01
5.00000E+00	-5.00000E+00	7.00000E+03	1.50561E-01
5.00000E+00	-5.00000E+00	7.60000E+03	1.50572E-01

Table 3

3 HDRL1C1N: Table 3 - Numerical Solution, Z=5m, T=100s

27 Number of lines to follow

1.00000E-01	-4.00000E+00	1.00000E+02	1.00000E+00
1.50000E-01	-4.00000E+00	1.00000E+02	8.75023E-01
2.00000E-01	-4.00000E+00	1.00000E+02	7.85848E-01
3.00000E-01	-4.00000E+00	1.00000E+02	6.61078E-01
4.00000E-01	-4.00000E+00	1.00000E+02	5.72357E-01
5.50000E-01	-4.00000E+00	1.00000E+02	4.75360E-01
7.00000E-01	-4.00000E+00	1.00000E+02	4.02849E-01
8.50000E-01	-4.00000E+00	1.00000E+02	3.45878E-01
1.00000E+00	-4.00000E+00	1.00000E+02	2.99562E-01
1.30000E+00	-4.00000E+00	1.00000E+02	2.28978E-01
1.60000E+00	-4.00000E+00	1.00000E+02	1.78252E-01
1.95000E+00	-4.00000E+00	1.00000E+02	1.35887E-01
2.30000E+00	-4.00000E+00	1.00000E+02	1.05759E-01
2.65000E+00	-4.00000E+00	1.00000E+02	8.40229E-02
3.00000E+00	-4.00000E+00	1.00000E+02	6.79881E-02
3.50000E+00	-4.00000E+00	1.00000E+02	5.16189E-02
4.00000E+00	-4.00000E+00	1.00000E+02	4.00470E-02
4.50000E+00	-4.00000E+00	1.00000E+02	3.15015E-02
5.00000E+00	-4.00000E+00	1.00000E+02	2.49267E-02
5.50000E+00	-4.00000E+00	1.00000E+02	1.97690E-02
6.00000E+00	-4.00000E+00	1.00000E+02	1.56354E-02
6.50000E+00	-4.00000E+00	1.00000E+02	1.23006E-02
7.00000E+00	-4.00000E+00	1.00000E+02	9.56602E-03
7.75000E+00	-4.00000E+00	1.00000E+02	6.33047E-03
8.50000E+00	-4.00000E+00	1.00000E+02	3.80637E-03
9.25000E+00	-4.00000E+00	1.00000E+02	1.76593E-03
1.00000E+01	-4.00000E+00	1.00000E+02	0.00000E+00

HYDROCOIN Level 1, Case 3

Calculation of saturated-unsaturated flow through a layered sequence of sedimentary rocks

Roger Thunvik
Royal Institute of Technology
Stockholm, Sweden

Contents

Nomenclature

symbol	description	dimension
c^f	compressibility of the fluid	$M^{-1}Lt^2$
c^r	compressibility of the rock matrix	$M^{-1}Lt^2$
g	acceleration of gravity	Lt^{-2}
k	permeability	L^2
p	pressure	$ML^{-1}t^{-2}$
q_i	specific flux	Lt^{-1}
Q	mass net infiltration rate	$ML^{-3}t^{-1}$
S	Saturation	-
S'	dS/dp	
t	time	t
T	temperature	T
u	volumetric rate of flow per unit area	Lt^{-1}
v	velocity	Lt^{-1}

Greek	description	dimension
β	coefficient of thermal volume expansion	T^{-1}
μ	dynamic viscosity	$ML^{-1}t^{-1}$
ρ	density	ML^{-3}
ϕ	porosity	-

superscripts

f	fluid
r	rock

Introduction

This case deals with unsaturated flow in a permeable medium. The problem was defined by Grundfeldt (1). A sedimentary rock formation containing some layers with different hydraulic properties is considered to define the present flow domain, which is modelled as a vertical cross-section. A schematic illustration of the flow domain and the various layers considered is given in Figure 1. The object is to determine the position of the water table using the parameter data according to the definition of the case (1).

The regions A and C are permeable relative to the host rock which is represented by region D. Region B is considered to be an aquitard between the regions A and C. Region E is assumed to be very pervious and should from a physical point of view partly be considered a seepage face. For a more detailed description of the background and assumptions on the flow domain see Grundfeldt (1).

Flow equations

The flow model used in the calculations was developed by Thunvik and Braester (3). The following equation for the conservation of mass of the fluid is considered in the calculations

$$(\phi S \rho^f)_{,t} - (\rho^f q_i)_{,i} + Q = 0 \tag{1}$$

where

$$q_i = -\frac{k}{\mu}_{ij} (p_{,j} - \rho^f g_j) \tag{2}$$

which is analogous to Darcy's law.

Fluid compressibility, rock compressibility and the coefficient of thermal volume expansion of the fluid are defined as

$$c^f = \frac{1}{\rho f} \frac{\partial \rho^f}{\partial p} \tag{3a}$$

$$c^r = \frac{1}{\phi} \frac{d\phi}{dp} \tag{3b}$$

$$\beta = -\frac{1}{\rho^f}\frac{\partial \rho^f}{\partial T^f} \tag{3c}$$

With these definitions the final form of the flow equation becomes

$$\phi\rho^f(S(c^f + c^r) + S')\, p_{,t} - \phi S\rho^f \beta\, T^f_{,t} +$$

$$-(\rho^f \frac{k}{\mu}_{ij}(p_{,j} - \rho^f g_j)_{,i} + Q = 0 \tag{4}$$

The flow equation is solved numerically using the Galerkin finite element method. The algebraic system of equations resulting from the Gauss integration over the elements is solved by Gauss elimination using the frontal method.

Boundary conditions

On top a prescribed flux condition corresponding to the net accretion as given in the specification report. The inclined lateral boundary should in principle be a seepage face. This type of boundary condition is difficult to treat properly in unsaturated flow models. Especially in cases where the position of the water table is unknown and if the flow conditions along the boundary may change from outflow to inflow as a result of accretion to the boundary. The lateral vertical boundary should represent a lake so hydrostatic pressure was set at this boundary according the elevation of the water table in the lake.

Assumptions

Some preliminary calculations showed that the flow problem is very difficult to solve using the original data in the report defining the problem. Therefore, the object of the present study was limited to seeking steady state solutions under simplifying assumptions. The most serious difficulties in the flow problem are thought to be associated with the extremely high permeability contrasts being encountered during some stages of the lowering of the water table.

The curves for the relative permeability in the the different media were therefore modified such that values less the 0.1 were never considered. The relationships between the relative permeability and saturation were modified such that the lowest relative permeability value used in the calculations was in the range between 0.1 and 0.25. The original curves for region A and C are shown in figure 3 and the original curves for regions B and D in Figure 4. The modified curves for region A and C are shown in Figure 5 and for regions B and D in Figure 6.

Input data

The following input parameter values were used in the calculations:

Table of input data

Symbol	Parameter	Value	Unit
fluid properties			
c^f	fluid compressibility	10^{-10}	Pa^{-1}
ρ^f	fluid density	1000	$kg\ m^{-3}$
μ	dynamic viscosity	10^{-3}	Pas
rock			
c^r	rock matrix compressibility	10^{-10}	Pa^{-1}
ϕ	porosity	0.03	-
k	rock permeability-medium A	10^{-14}	m^2
	rock permeability-medium B	10^{-16}	m^2
	rock permeability-medium C	10^{-14}	m^2
	rock permeability-medium D	10^{-10}	m^2
	rock permeability-medium D	10^{-12}	m^2
Boundary condition on top of medium A			
Q	net accretion	$3.17\ 10^{-9}$	ms^{-1}

Results

Initially, hydrostatic conditions were assumed to prevail in the flow domain and the water table (atmospheric pressure) was assumed to be located just below the ground surface.

Usually, the solutions could be advanced 10-15 time steps without much problem to a situation with the water table located at about 375 metres on the left hand side (see Figure 7). Further advance in time of the solution appeared to be very difficult. In fact the solution could be totally destroyed within a single time step after this position.

In a first attempt to reach a steady state solution to the problem the relative permeability was set equal to one for all saturations and with the water table located at about 375 metres on the left hand side. As a result the solution could readily be advanced to steady state and the water table reached a position of the water table at about 65 metres on the left hand side. This situation is shown in Figure 8.

In a second attempt to reach steady state the minimum value of the relative permeability was set equal to 0.25 when the water table on the left hand side was located at 375 metres. The solution could now be advanced fairly easy to a steady state position with the water table at a level of about 220 metres on the left hand boundary. The water table is thus entirely located below the aquitard. This situation is graphically displayed in Figure 9. Some oscillatory behaviour of the water table on the left hand boundary could be observed, but the final flow conditions appeared to be quite stable.

In a third attempt to reach steady state the conditions were the same as for in the second attempt, but the solution was advanced using much smaller time steps in order to avoid the oscillatory behaviour on the left hand boundary. In this case steady state conditions were achieved with the water table located above the aquitard on the left hand boundary. The solution is depicted in Figure 10.

Also Noy (2) reported different steady state positions of the water table when using different characteristic curves for the unsaturated hydraulic conditions. It is not yet clear, however, whether the contradictions in the solutions obtained here are realistic or simply the result of improper numerical treatment of the problem.

Generally, it may be concluded from the previous calculations that the problem exactly as defined in the specification document could not be solved with the present version of the computer model used in the calculations (3). Furthermore, it may be concluded that simplifying assumptions such as those made in the calculations may change the behaviour of the flow problem and lead to erroneous solutions.

Among the features that need be developed or implemented in the present numerical model to facilitate the treatment of unsaturated flow could be mentioned time step control algoritms and mesh adaptive techniques.

References

1. Grundfeldt, Bertil, 1984, Proposal for a test problem for Hydrocoin Level 1, Case 3, saturated-unsaturated flow through a layered sequence of sedimentary rocks, Kemakta Consultants Co.
2. Noy, David, 1985, Hydrocoin newsletter, 1985-07-16, Optional extra calculations for Level 1, Case 3, BGS.
3. Thunvik,R. and Braester, C., 1980, Hydrothermal conditions around a radioactive waste repository, Part 1 - A mathematical model for the flow of groundwater and heat in fracture rock, part 2 - Numerical solutions, Part 3 - Numerical solutions for anisotropy, SKBF-KBS-TR:80-19.
4. Thunvik, Roger, 1984, Calculations of fluxes through a repository caused by a local well, SKBF.KBS-TR:83-50.

Figures

Figure 1. Sketch of flow domain (vertical section).

Figure 2. Element grid.

Figure 3. Capillary pressure verus saturation and relative permeability versus saturation for regions A and C (original curves).

Figure 4. Capillary pressure verus saturation and relative permeability versus saturation for regions B and D (original curves).

Figure 5. Capillary pressure verus saturation and relative permeability versus saturation for regions A and C (modified curves).

Figure 6. Capillary pressure verus saturation and relative permeability versus saturation for regions B and D (modified curves).

Figure 7. Results for the position of the water table at various points of the time. During the first stage (the water table on the left hand boundary being lowered from about 500 to 375 m) the relative permeability was in the range from 0.1 to 1.0. During the second stage (the water table on the left hand boundary being lowered from about 375 to 65 m) the relative permeability was 1.0 until steady state was reached.

Figure 8. Results for the position of the water table at various points of the time. During the first stage (the water table on the left hand boundary being lowered from about 500 to 375 m) the relative permeability was in the range from 0.1 to 1.0. During the second stage (the water table on the left hand boundary being lowered from about 375 to 220 m) the relative permeability was from 0.25 to 1.0 until steady state was reached.

Figure 9. Results for the position of the water table at various points of the time. During the first stage (the water table on the left hand boundary being lowered from about 500 to 375 m) the relative permeability was in the range from 0.1 to 1.0. During the second stage (the water table on the left hand boundary being lowered from about 375 to 320 m) the relative permeability was from 0.25 to 1.0 until steady state was reached.

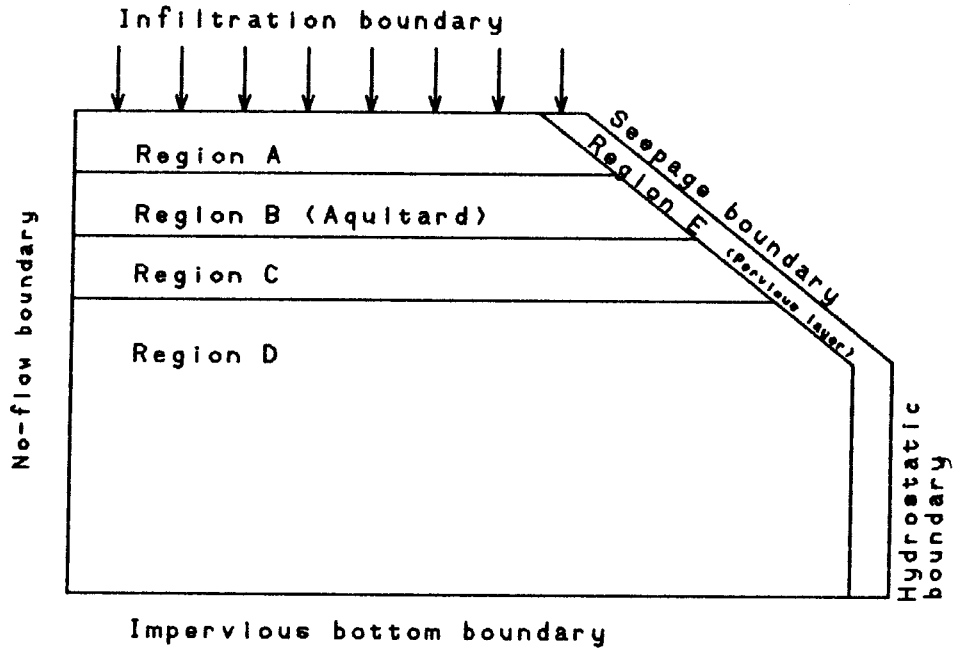

Figure 1. Schematic illustration of flow domain

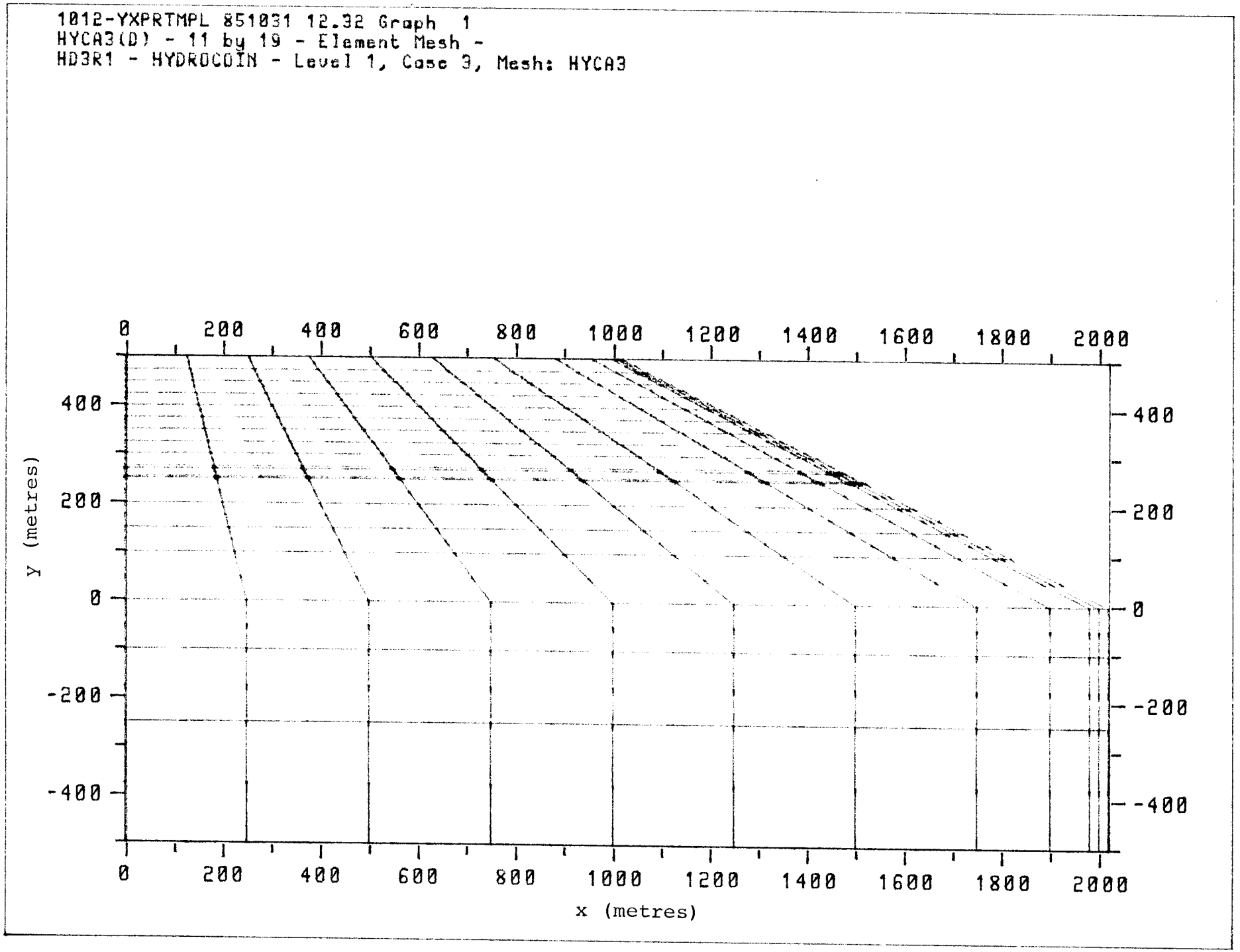
1012-YXPRTMPL 851031 12.32 Graph 1
HYCA3(D) - 11 by 19 - Element Mesh -
HD3R1 - HYDROCOIN - Level 1, Case 3, Mesh: HYCA3
0
200
400
600
800
1000
1200
1400
1600
1800
2000
400
200
0
-200
-400
y (metres)
x (metres)

Figure 2.

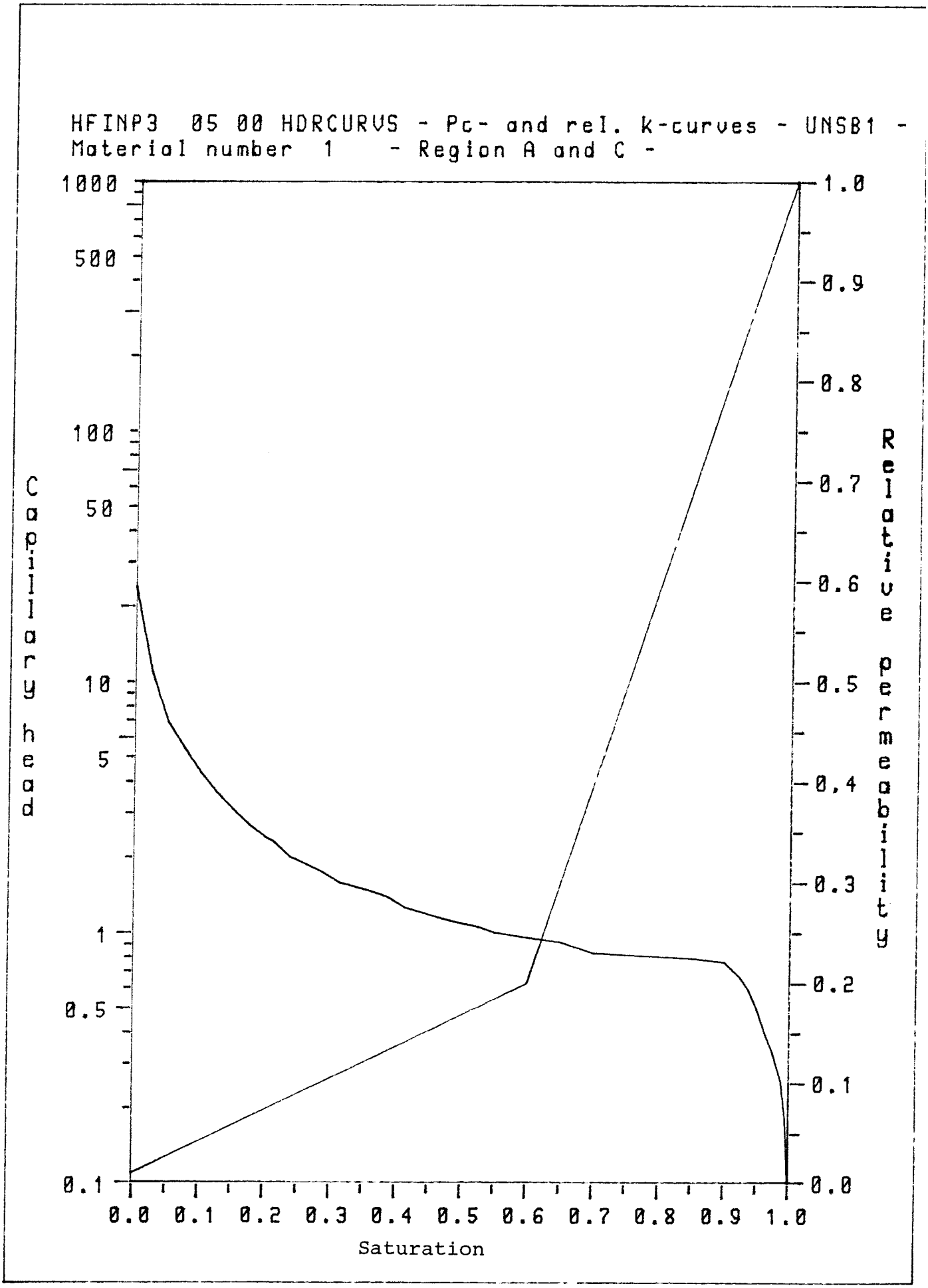
HFINP3 05 00 HDRCURVS - Pc- and rel. k-curves - UNSB1 -
Material number 1 - Region A and C -
1000
500
100
50
10
5
1
0.5
0.1
Capillary head
1.0
0.9
0.8
0.7
0.6
0.5
0.4
0.3
0.2
0.1
0.0
Relative permeability
0.0 0.1 0.2 0.3 0.4 0.5 0.6 0.7 0.8 0.9 1.0
Saturation

Figure 3.

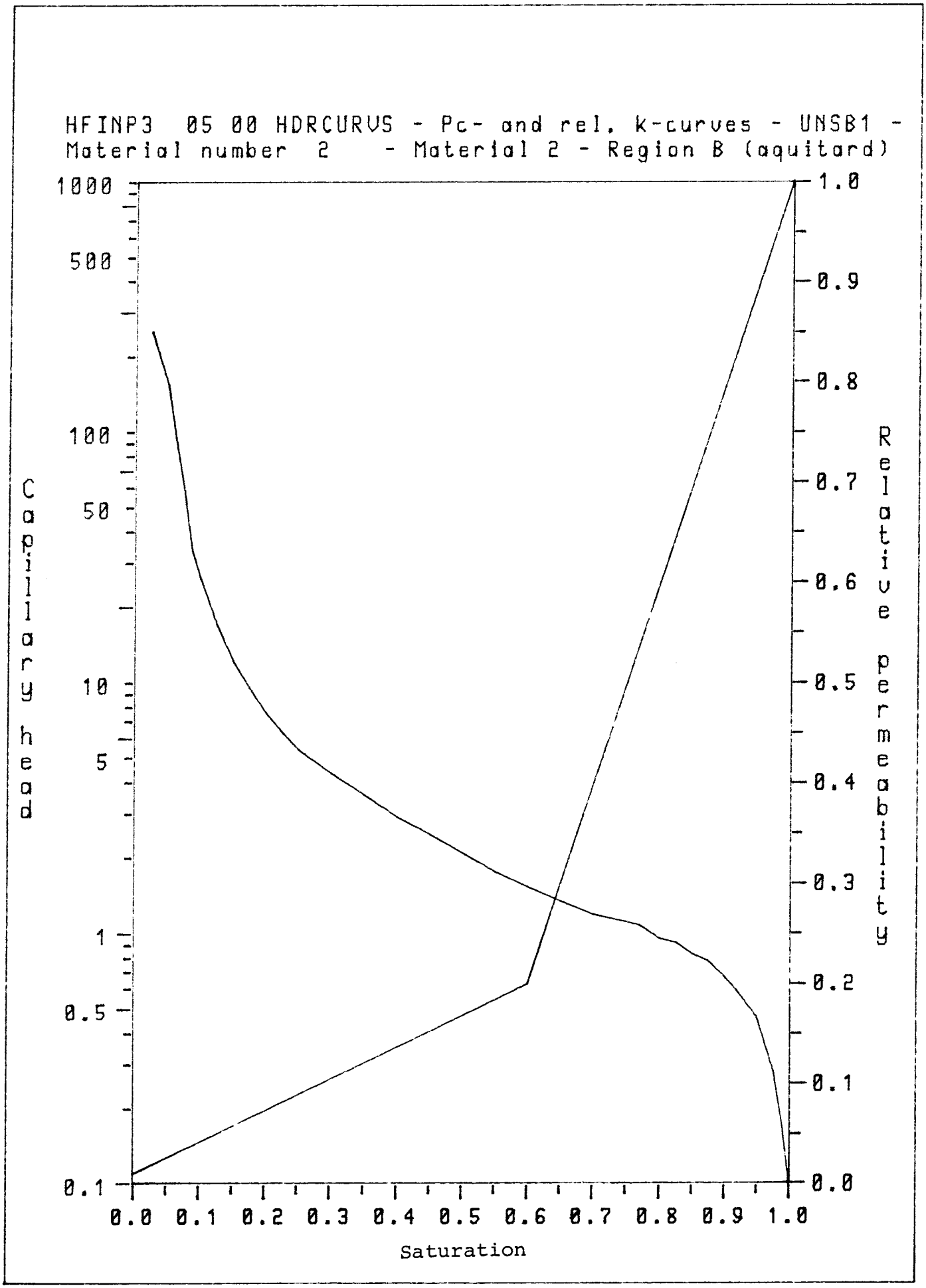
HFINP3 05 00 HDRCURVS - Pc- and rel. k-curves - UNSB1 -
Material number 2 - Material 2 - Region B (aquitard)
1000
500
100
50
10
5
1
0.5
0.1
Capillary head
1.0
0.9
0.8
0.7
0.6
0.5
0.4
0.3
0.2
0.1
0.0
Relative permeability
0.0 0.1 0.2 0.3 0.4 0.5 0.6 0.7 0.8 0.9 1.0
Saturation

Figure 4.

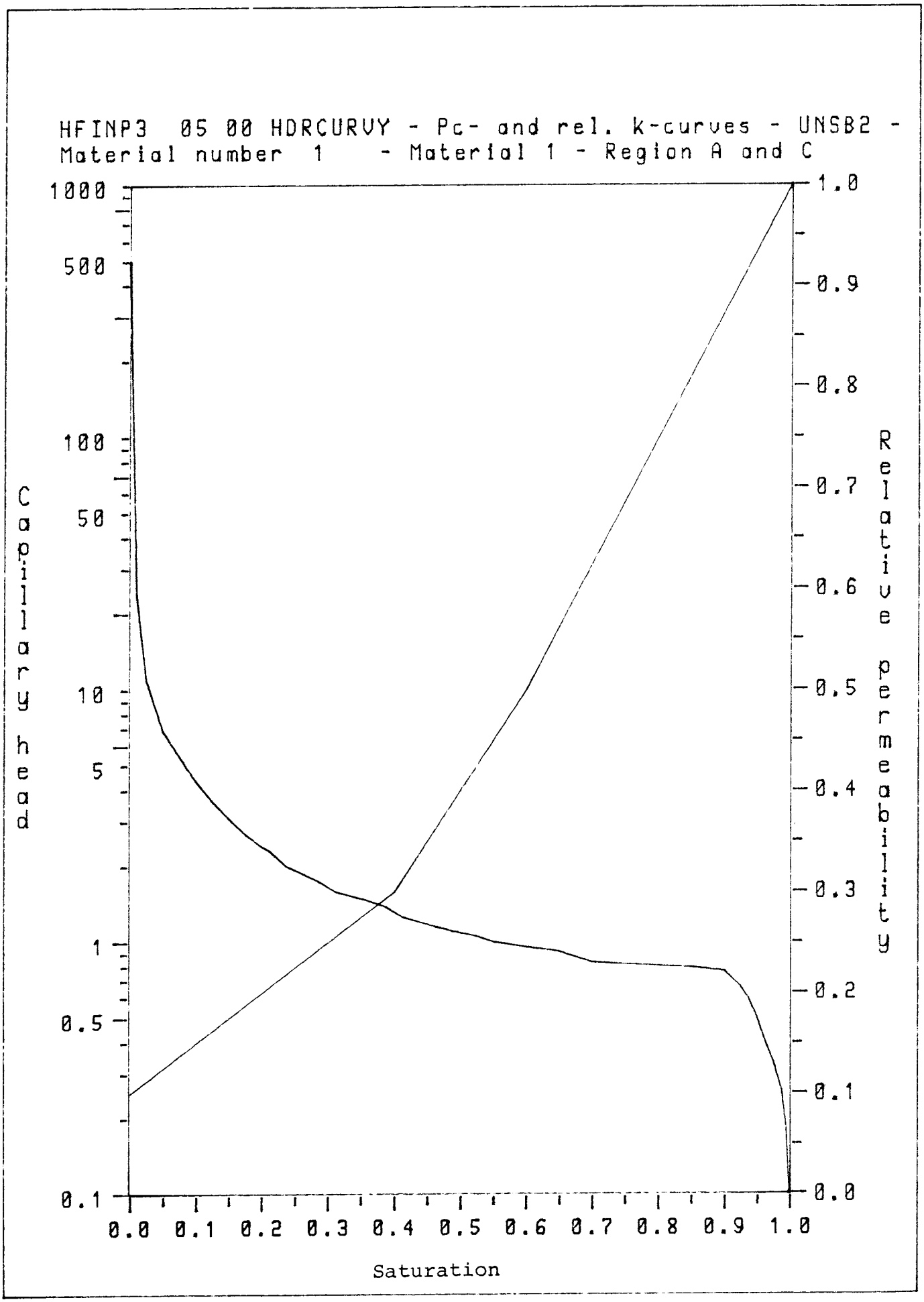
HFINP3 05 00 HDRCURVY - Pc- and rel. k-curves - UNSB2 -
Material number 1 - Material 1 - Region A and C
1000
500
100
50
10
5
1
0.5
0.1
Capillary head
1.0
0.9
0.8
0.7
0.6
0.5
0.4
0.3
0.2
0.1
0.0
Relative permeability
0.0 0.1 0.2 0.3 0.4 0.5 0.6 0.7 0.8 0.9 1.0
Saturation

Figure 5.

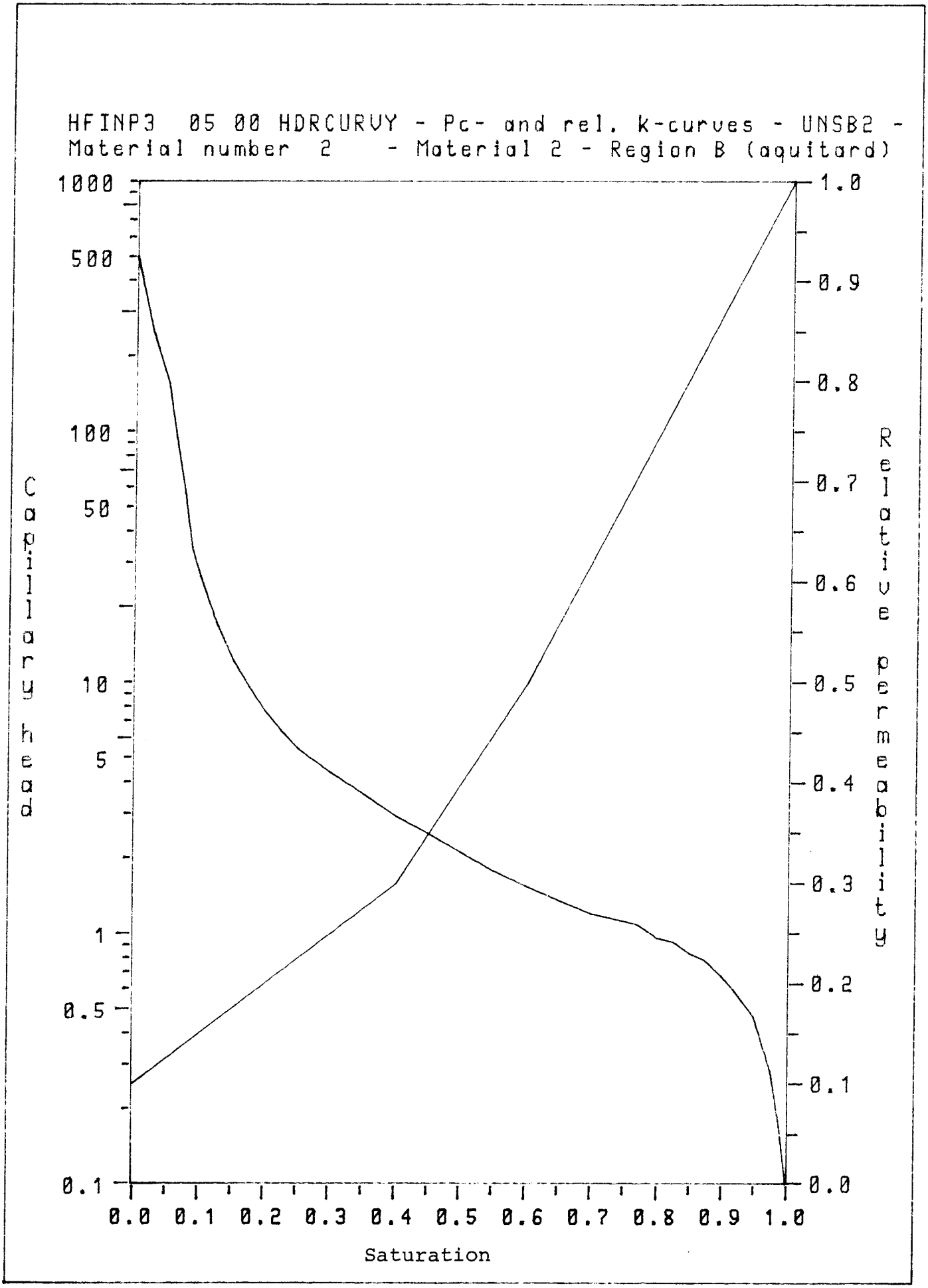
HFINP3 05 00 HDRCURVY - Pc- and rel. k-curves - UNSB2 -
Material number 2 - Material 2 - Region B (aquitard)
1000
500
100
50
10
5
1
0.5
0.1
Capillary head
1.0
0.9
0.8
0.7
0.6
0.5
0.4
0.3
0.2
0.1
0.0
Relative permeability
0.0 0.1 0.2 0.3 0.4 0.5 0.6 0.7 0.8 0.9 1.0
Saturation

Figure 6.

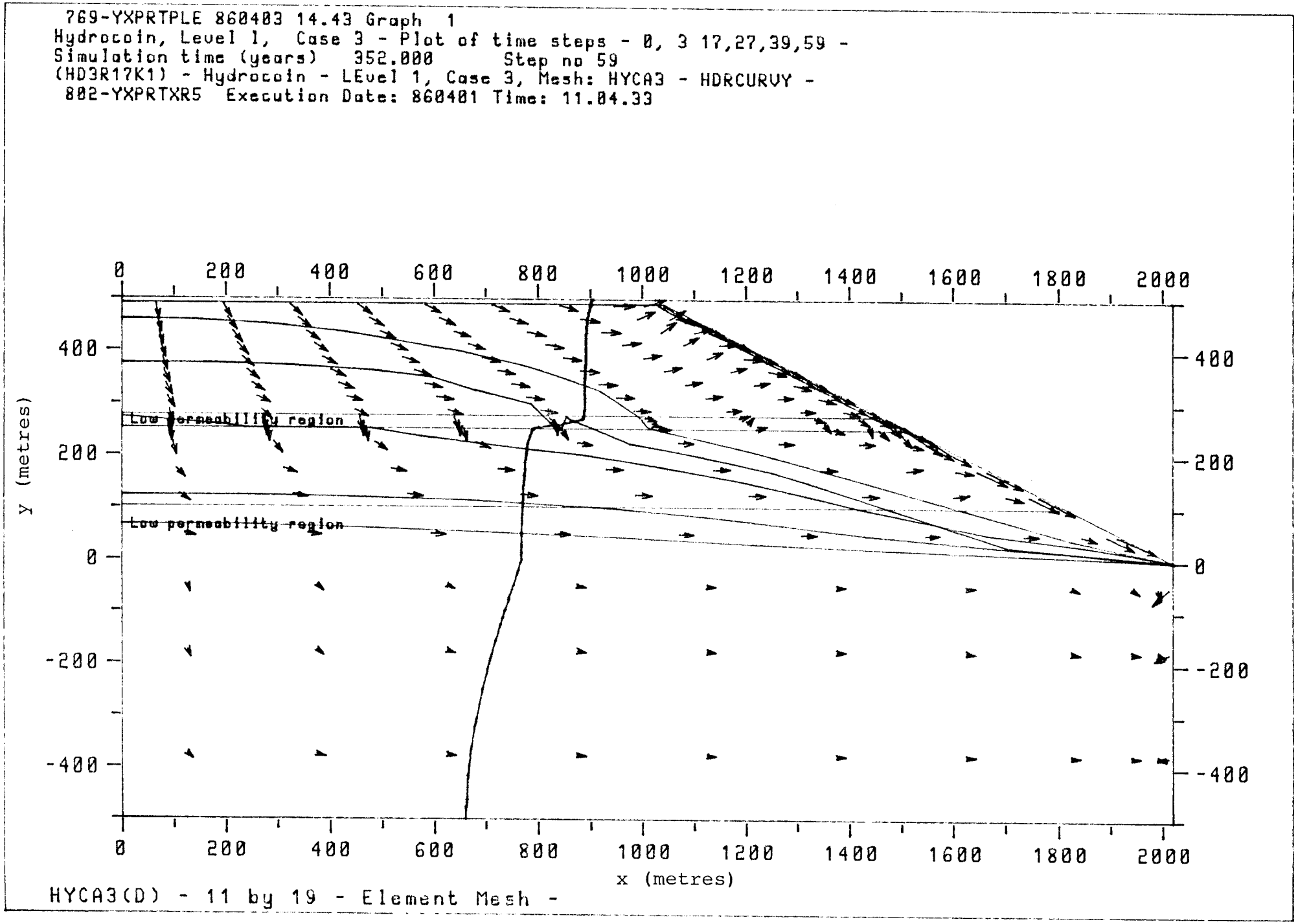
769-YXPRTPLE 860403 14.43 Graph 1
Hydrocoin, Level 1, Case 3 - Plot of time steps - 0, 3 17,27,39,59 -
Simulation time (years) 352.000 Step no 59
(HD3R17K1) - Hydrocoin - LEvel 1, Case 3, Mesh: HYCA3 - HDRCURVY -
802-YXPRTXR5 Execution Date: 860401 Time: 11.04.33
Low permeability region
Low permeability region
y (metres)
x (metres)
0
200
400
600
800
1000
1200
1400
1600
1800
2000
-200
-400
HYCA3(D) - 11 by 19 - Element Mesh -

Figure 7.

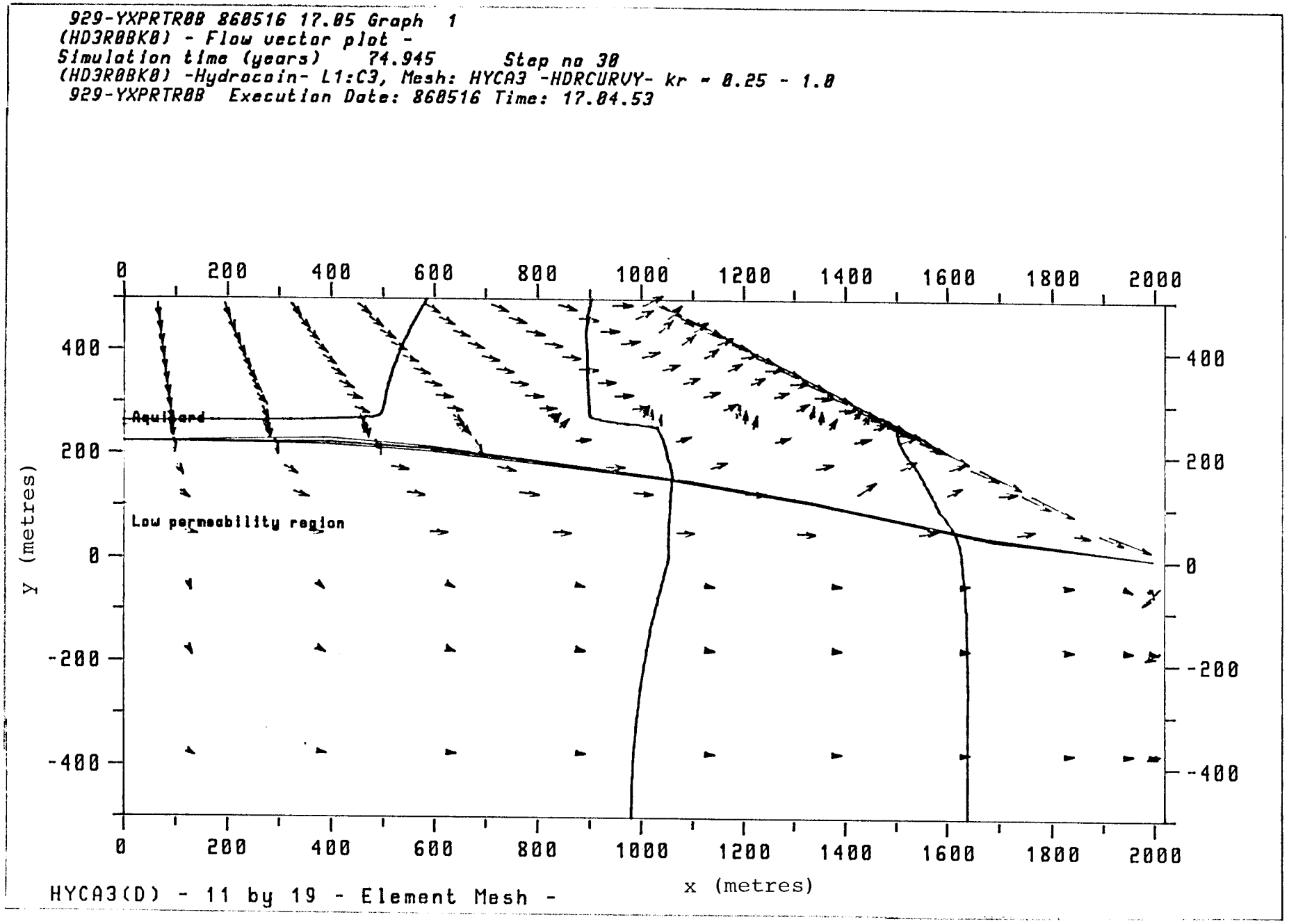
929-YXPRTR0B 860516 17.05 Graph 1
(HD3R0BK0) - Flow vector plot -
Simulation time (years) 74.945 Step no 30
(HD3R0BK0) -Hydrocoin- L1:C3, Mesh: HYCA3 -HDRCURVY- kr = 0.25 - 1.0
929-YXPRTR0B Execution Date: 860516 Time: 17.04.53
Aquitard
Low permeability region
y (metres)
x (metres)
HYCA3(D) - 11 by 19 - Element Mesh -

Figure 8.

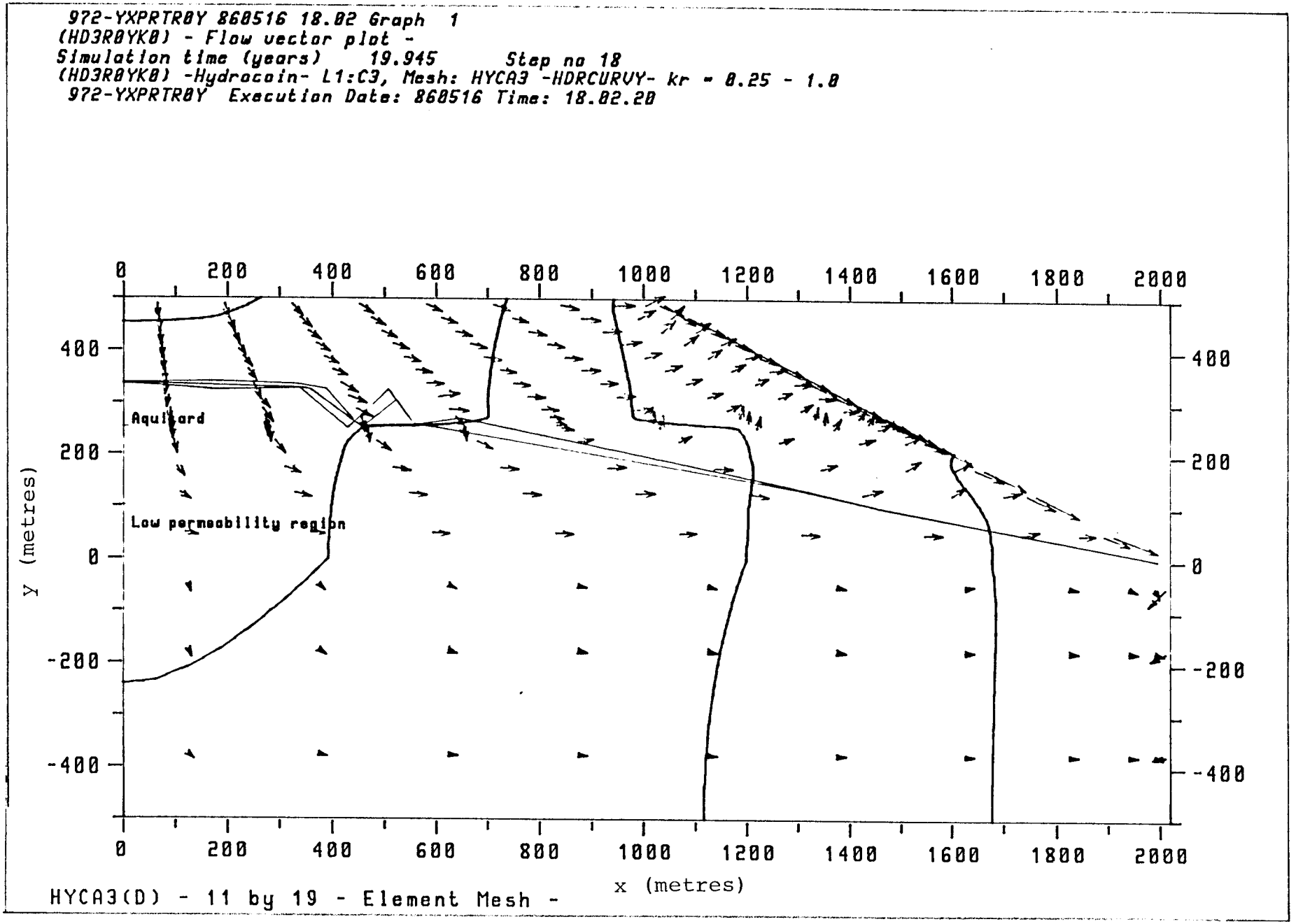
972-YXPRTR0Y 860516 18.02 Graph 1
(HD3R0YK0) - Flow vector plot -
Simulation time (years) 19.945 Step no 18
(HD3R0YK0) -Hydrocoin- L1:C3, Mesh: HYCA3 -HDRCURVY- kr = 0.25 - 1.0
972-YXPRTR0Y Execution Date: 860516 Time: 18.02.20
Aquitard
Low permeability region
y (metres)
x (metres)
HYCA3(D) - 11 by 19 - Element Mesh -

Figure 9.

HYDROCOIN Level 1, Case 4

Calculation of transient thermal convection in a saturated medium

Roger Thunvik

Rina Rotshild

Royal Institute of Technology

Stockholm, Sweden

Contents

Introduction

This case deals with transient thermal convection in a saturated permeable medium. The test problem was defined by Hodgkinson(1). An analytical solution was also presented and the numerical results worked out in the present study are presented together with the analytical solution. A schematic illustration of the flow problem considered is given in Figure 1.

The purpose of this case is to calculate time dependent buoyancy driven flows due to heat released from a hypothetical radioactive waste repository. The problem is characterized by a low Rayleigh number and it is assumed that the heat flow is mainly due to conduction. The repository is represented by a spherical heat source, which is exponentially decaying with time. The surrounding rock mass is assumed to be homogeneous and isotropic. The same material properties are assumed for the repository as for the surrounding rock mass.

Flow model

The flow model used in the calculation was developed by Thunvik and Braester (2). The following set of equations is used in the calculations

$$\phi\rho^f (c^f + c^r)\, p_{,t} - \phi\rho^f \beta T^f_{,t} - (\rho^f \underline{\underline{k}}_{\mu} ij\, (p_{,j} - \rho^f g_j) = 0$$

$$(\rho C)^*\, T_{,t} - (\lambda^*\, T_{,j})_{,j} + Q = 0$$

where ϕ is porosity, ρ^f is fluid density, c^f is fluid compressibility, c^f is rock compressibility, β is coefficient of thermal volume expansion, T is temperature, k_{ij} is the permeability tensor, μ is dynamic viscosity, p is pressure and g is the acceleration of gravity. In the heat flow equation $(\rho C)^*$ was defined as

$$(\rho C)^* = \phi\rho^f C^f + (1-\phi)\rho^r C^r$$

and

$$(\rho C)^* = \phi\lambda^f + (1-\phi)\,\lambda^r C^f$$

where λ^f is the thermal conductivity.

The flow equation is solved numerically using the Galerkin finite element method. The algebraic system of equations resulting from the Gauss integration over the elements is solved by Gauss elimination using the frontal method.

Boundary conditions

Initially pressure and temperature were set equal to zero all over the flow domain. No-flow boundary conditions were set both for the fluid and the heat flow.

Input data

The heat source was input as a distributed heat source with a strength (w_o) of

$$w_o = Q/V = Q_o/(4\pi r^3/3)$$

The solution was worked out using a mesh of 216 elements and 715 nodes. The mesh used is shown in Figure 2 and 3. The element mesh was densified around the edge of the heat source and a smooth variation of the heat source was applied to describe better the transition to the surrounding rock mass and to avoid overestimation of the total load of the hypothetical repository.

The element mesh was constructed by transforming a rectangular grid mesh into a half circle. The radial extent of the flow domain was 3000 metres. Only 8-node quadri-lateral elements were considered. Therefore, a small opening was left at the centre of the domain. The decay function was

$$w = w_o\, e^{-\alpha t}$$

where α is the decay constant.

Results

Solutions were worked out refining the discretization of the element mesh until it could be observed from the graphical displays that the numerical results were in good agreement with the analytical solutions for pressure and temperature. The results of the calculations for temperature and dynamic pressure are shown in Figures 4-7. Pathlines were also evaluated, but only the short term pathlines could be predicted in a reliable way.

The main predicted variables in the flow model are pressure and temperature. Therefore, pathline tracking is performed by post-processing of the solution data at successive time intervals. Rather large time steps were used to obtain the long term solutions.

No particular problems because of the large time steps used could be observed in the solutions for temperature and pressure being the variables considered for judging the quality of the results. However, numerical problems arose when performing pathline tracking in the long term flow fields and it was found that too large time steps had been used in the calculations.

In addition to the numerical problems associated with the discretization of the time domain as well as the flow domain, there is also a numerical problem associated with the representation of the flow velocity. Velocity is evaluated using Darcy's law

$$v = \frac{k}{\phi\mu}_{ij} (p_{,j} - \rho^f g_j)$$

In the present numerical formulation the same basis functions are used to evaluate the pressure gradient as well as the fluid density in the previous equation. In consequence, the representation of the flow velocity will be inconsistent.

Obviously, the results of the pathlines could be improved by simply increasing the resolution of the time domain as well as the flow domain and to change the boundary condition for the fluid to prescribed zero pressure instead of prescribed zero flux as was used in the calculations. It was concluded that in order to make it worthwhile the effort of re-calculating the present case that also the inconsistency problem should be taken care of in the calculations.

Table of input data

Symbol	Parameter	Value	
A	Radius of repository sphere	250.0	m
Q_o	Initial total power input	10.0	MW
w_o	Initial distributed heat source	0.15289	$W\ m^{-3}$
α	Decay constant	$7.322*10^{-10}$	s^{-1}
ϕ	Porosity	0.0001	
rock			
λ	Thermal conductivity	2.51	$Wm^{-1}K^{-1}$
ρ^r	Density	2.600	kgm^{-3}
	Specific heat capacity	879	$Jkg^{-1}K^{-1}$
k	Permeability	10^{-16}	m^2
water			
ρ^f	Density	992.2	kg^{-3}
β	Expansion coefficient	$3.85*10^{-4}$	K^{-1}
μ	Dynamic viscosity	$6.529*10^{-4}$	$kgm^{-1}s^{-1}$

References

1. Hodgkinson,D., 1985, Specification of a test problem for Hydrocoin Level 1 Case 4: Transient thermal convection in a saturated permeable medium, AERE -R - 11566, DOE/RW/84.198.
2. Thunvik,R. and Braester, C., 1980, Hydrothermal conditions around a radioactive waste repsitory, Part 1 - A mathematical model for the flow of groundwater and heat in fracture rock, part 2 - Numerical solutions, Part 3 - Numerical solutions for anisotropy, SKBF-KBS-TR:80-19.

List of figures

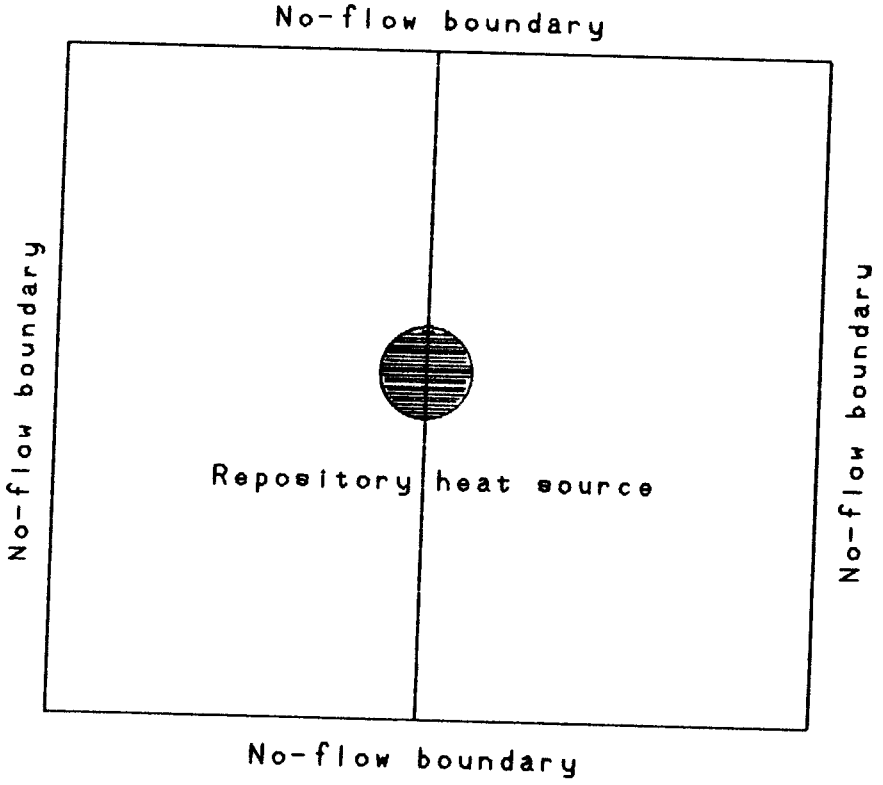

Figure 1. Schematic illustration of the flow problem

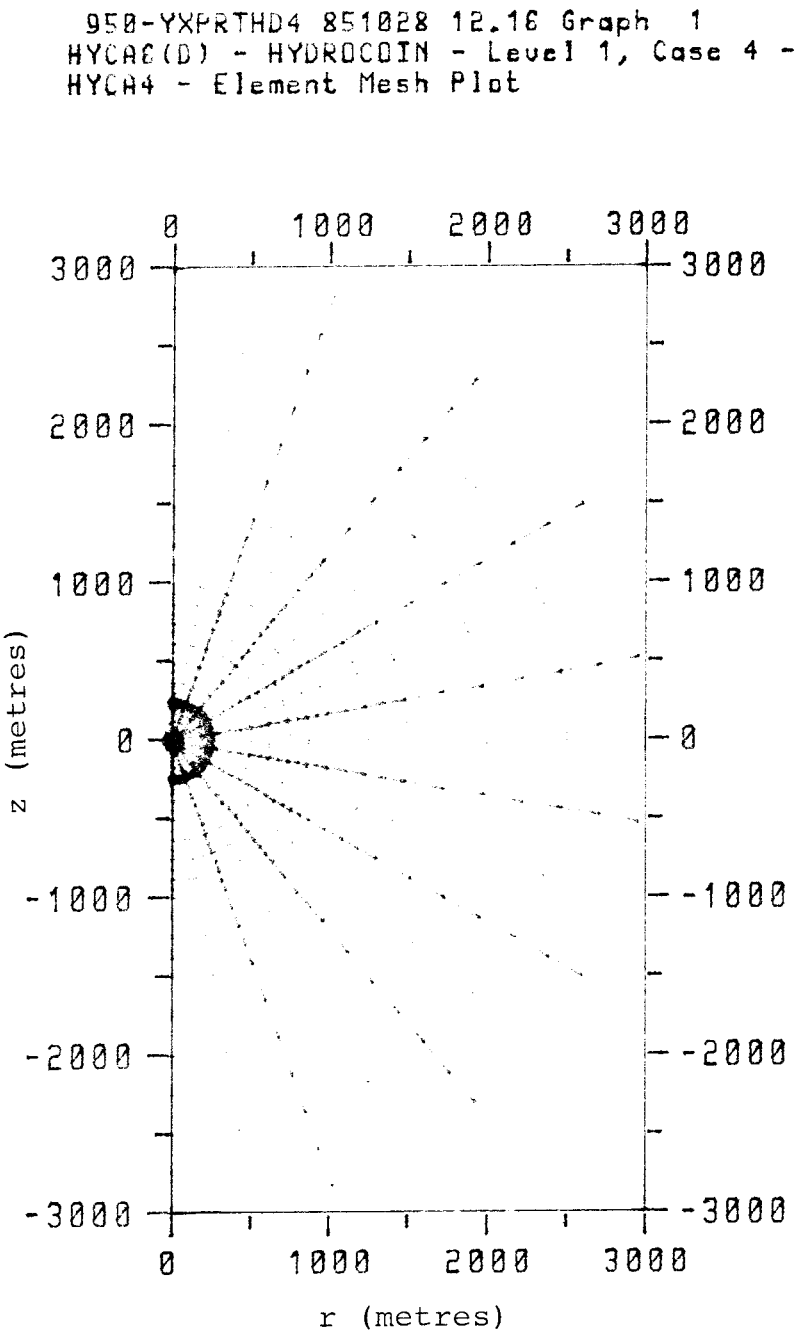

Figure 2. Element grid used in the calculations.

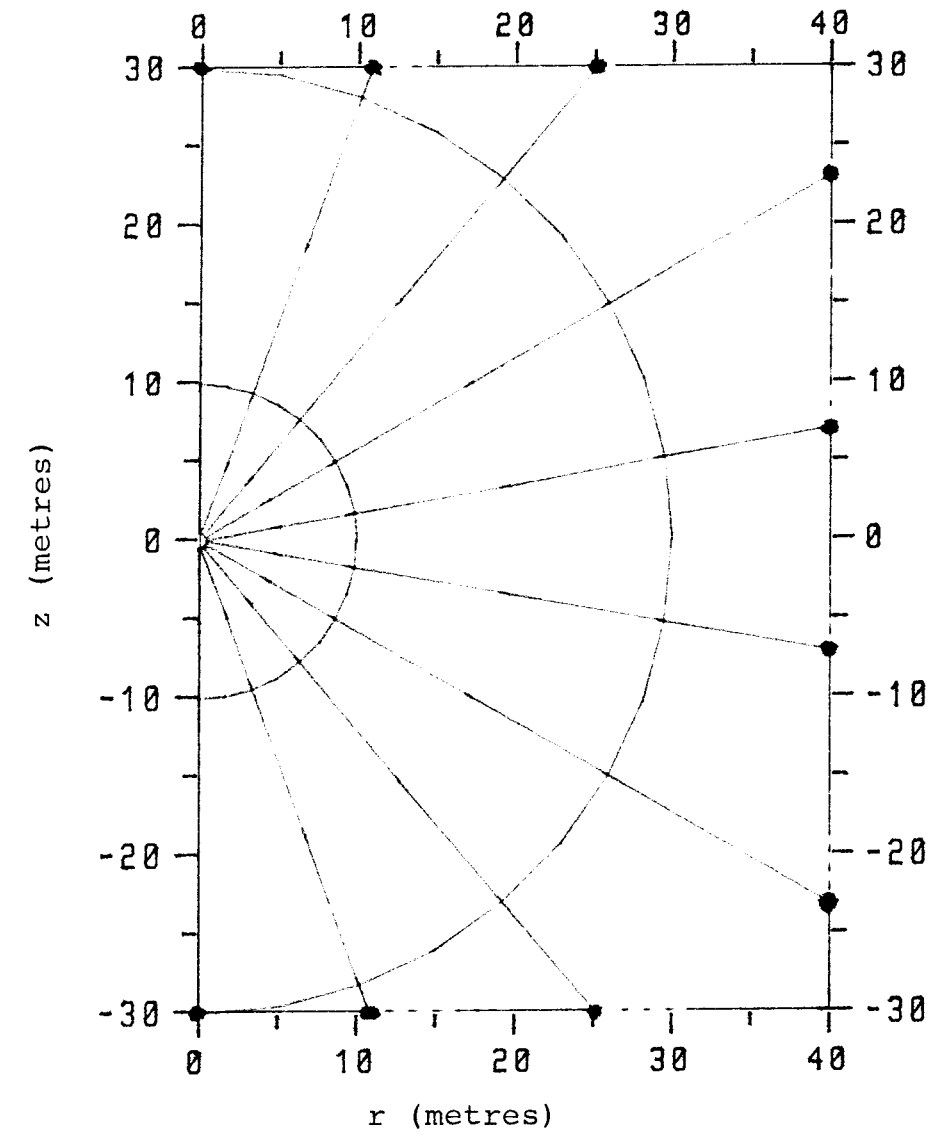

Figure 3. Centre part of the element grid.

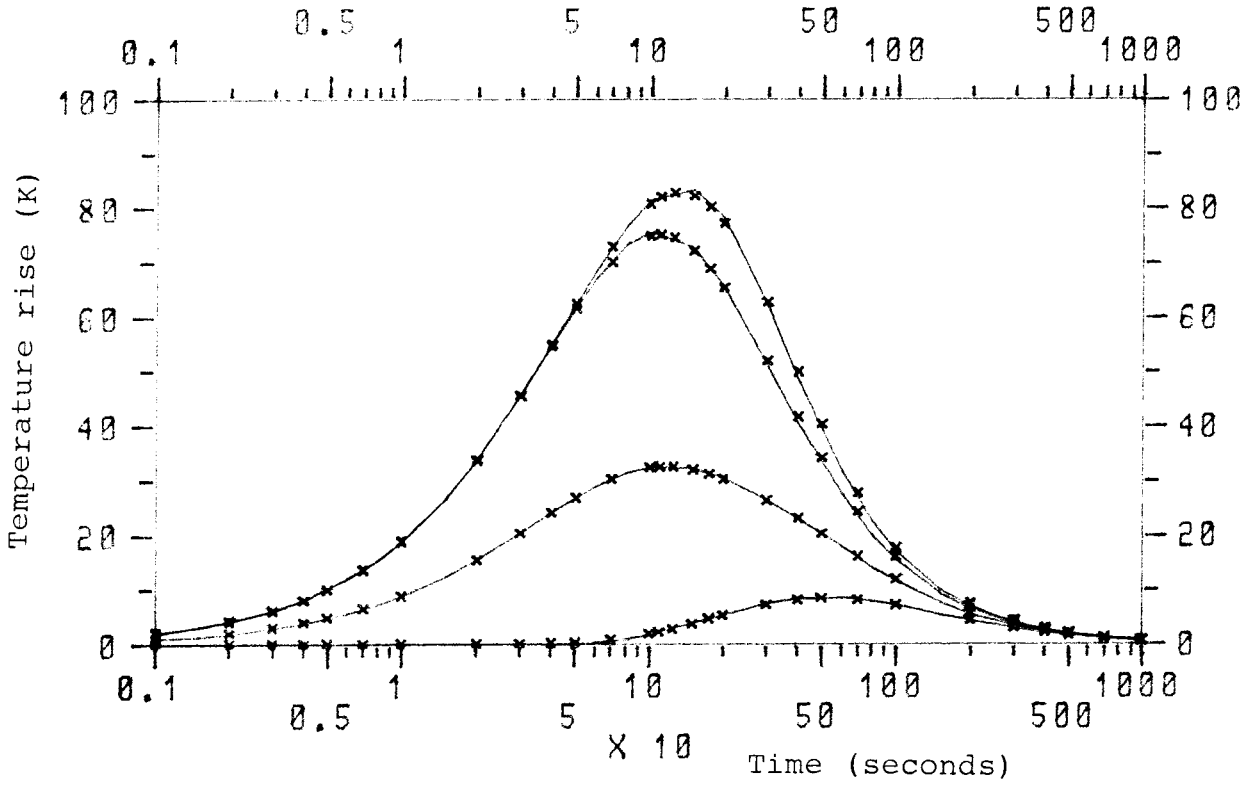

Figure 4.

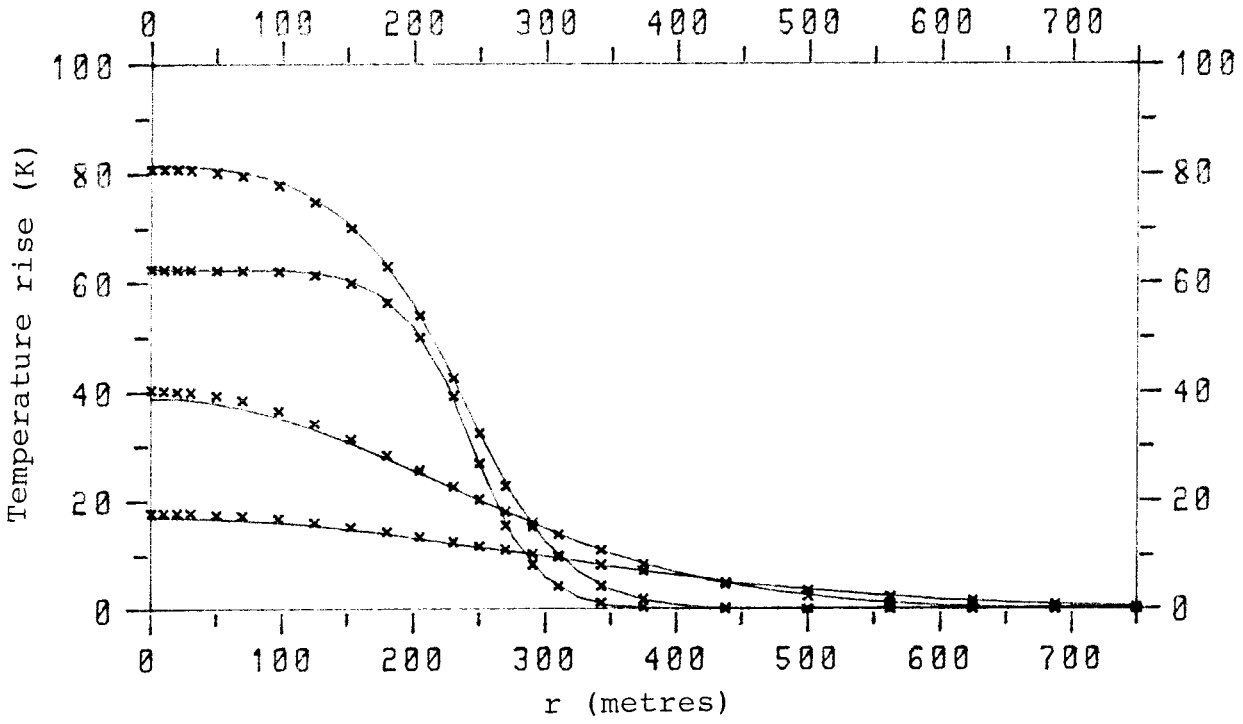

Figure 5.

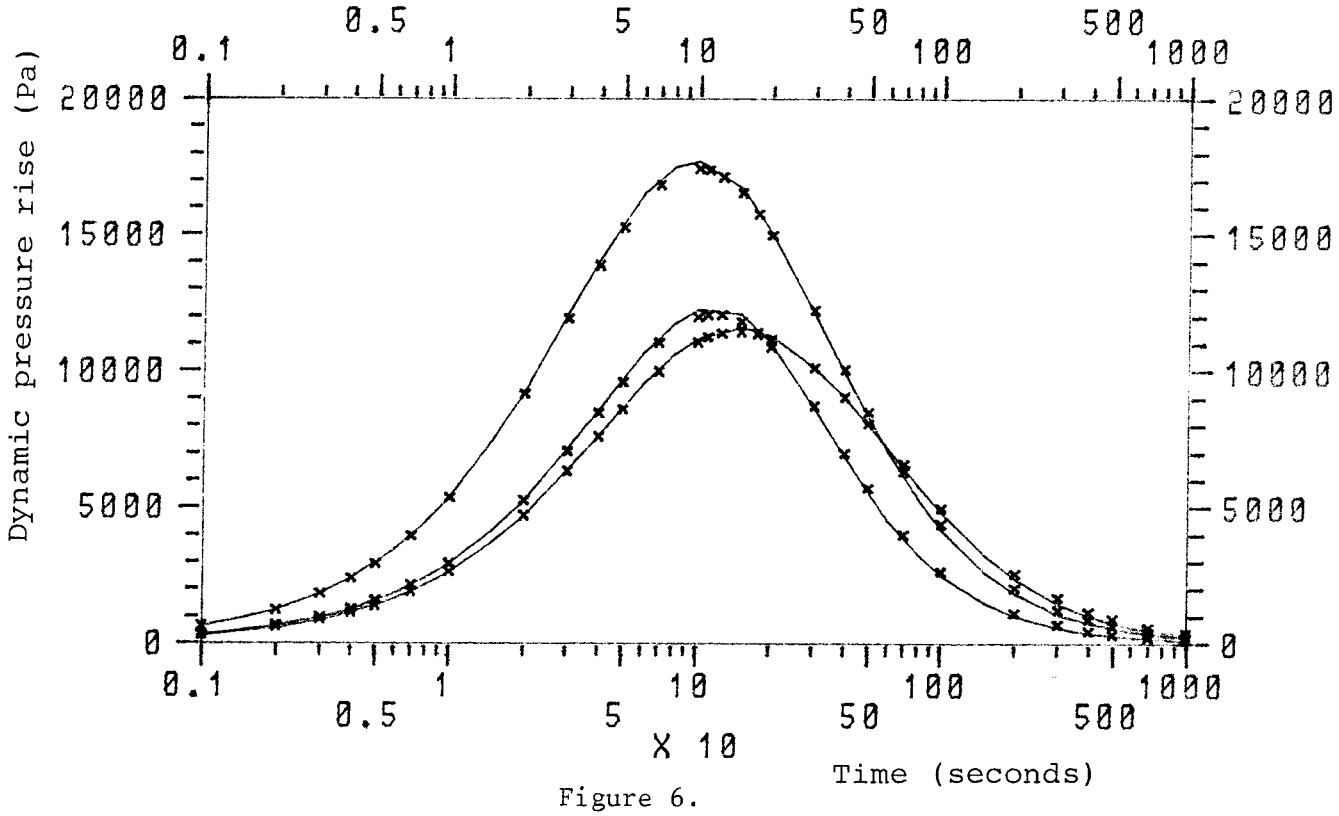

Figure 6.

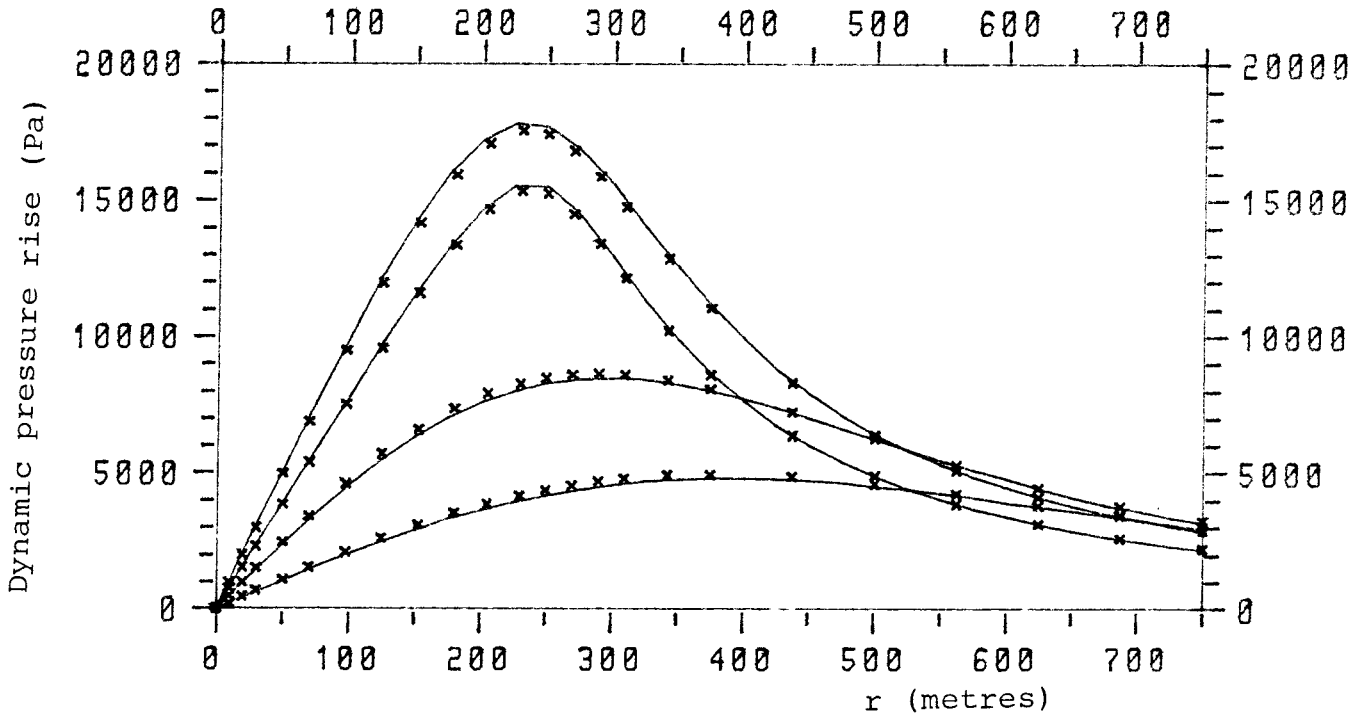

Figure 7.

1786-YXPRTPT1 850916 9.50 GRAPH 1
HDGR1 - Pathline Trace - Ts= 100 Years

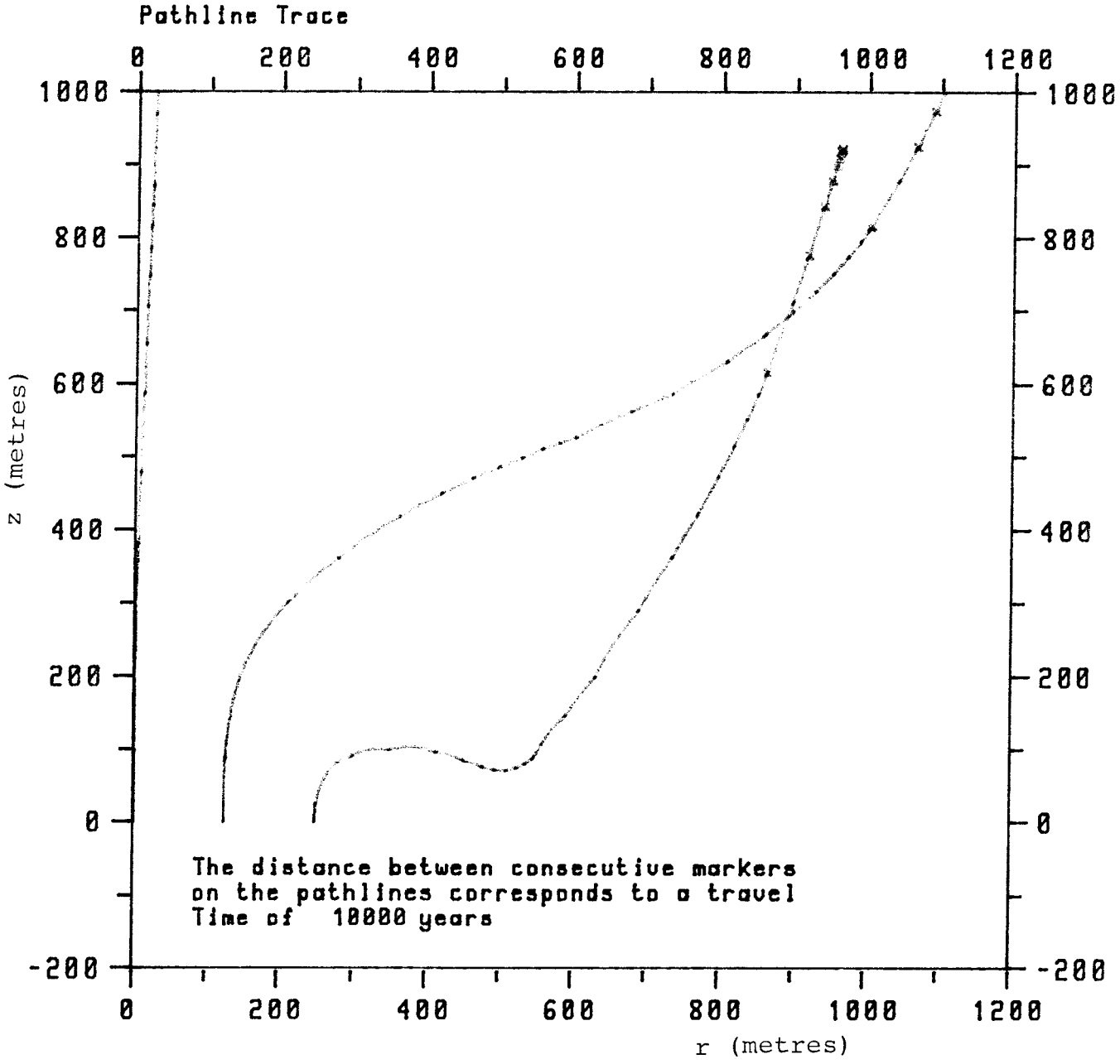

Figure 8.

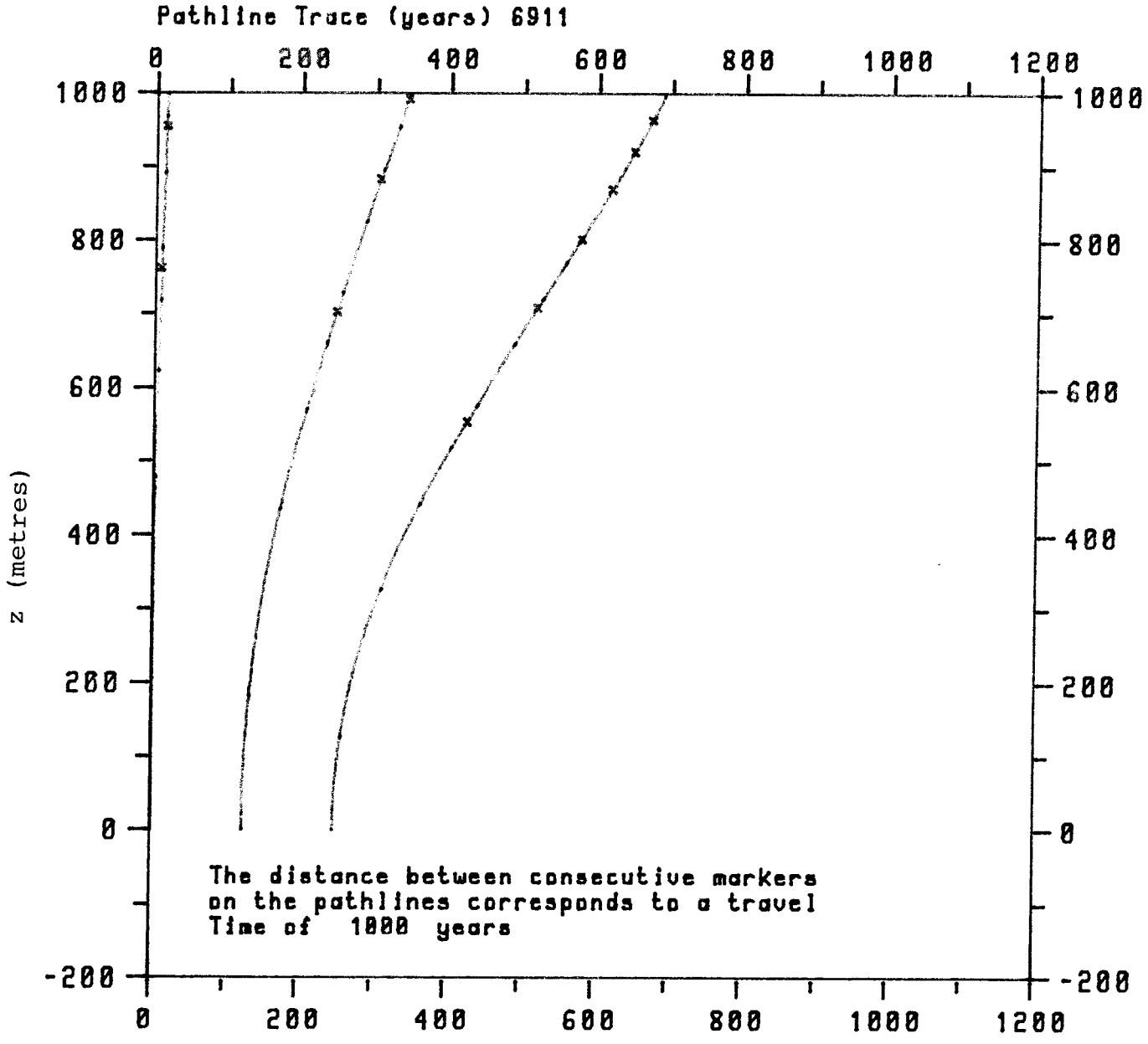
124-YXPRTPT2 850927 9.18 GRAPH 1
HD4R1 - Pathline Trace - Ts= 1000 Years
Pathline Trace (years) 6911
0
200
400
600
800
1000
1200
z (metres)
r (metres)
The distance between consecutive markers
on the pathlines corresponds to a travel
Time of 1000 years

Figure 9.

Appendix: Tables of results submitted to the project secreteriat

Table 1. Time dependent temperature and dynamic pressure rises along the vertical centre line (r=0) at z= 0 metres.

Table 2. Time dependent temperature and dynamic pressure rises along the vertical centre line (r=0) at z= 125, metres.

Table 3. Time dependent temperature and dynamic pressure rises along the vertical centre line (r=0) at z= 250 metres.

Table 4. Time dependent temperature and dynamic pressure rises along the vertical centre line (r=0) at z= 375 metres.

Table 5. Temperature and dynamic pressure rise profiles along the vertical centre line (r=0) at 50 years.

Table 6. Temperature and dynamic pressure rise profiles along the vertical centre line (r=0) at 100 years.

Table 7. Temperature and dynamic pressure rise profiles along the vertical centre line (r=0) at 500 years.

Table 8. Temperature rise and dynamic pressure rise profiles along the vertical centre line (r=0) at 1000 years.

Table 9. Pathlines starting at t_s=100 years.

Pathlines starting at t_s=1000 years.

Pathlines starting at t =10000 years.

Table 1

1 HDRL1C4N: Numerical Solution for Time-dep. T and P at R=Z=0

37 Number of lines to follow

5.00000E-01	2.50000E-01	5.25918E-01	2.57695E-01
5.00000E-01	5.00000E-01	1.04881E+00	5.13900E-01
5.00000E-01	1.00000E+00	2.08556E+00	1.02161E+00
5.00000E-01	2.00000E+00	4.12348E+00	2.01851E+00
5.00000E-01	3.00000E+00	6.11485E+00	2.99130E+00
5.00000E-01	4.00000E+00	8.06070E+00	3.94072E+00
5.00000E-01	5.00000E+00	9.96211E+00	4.86740E+00
5.00000E-01	7.00000E+00	1.36356E+01	6.65481E+00
5.00000E-01	1.00000E+01	1.88372E+01	9.17911E+00
5.00000E-01	2.00000E+01	3.37831E+01	1.63894E+01
5.00000E-01	3.00000E+01	4.56403E+01	2.20655E+01
5.00000E-01	4.00000E+01	5.50433E+01	2.65419E+01
5.00000E-01	5.00000E+01	6.24622E+01	3.00610E+01
5.00000E-01	7.00000E+01	7.28383E+01	3.49676E+01
5.00000E-01	1.00000E+02	8.07873E+01	3.87202E+01
5.00000E-01	1.10000E+02	8.20341E+01	3.93096E+01
5.00000E-01	1.25000E+02	8.28972E+01	3.97200E+01
5.00000E-01	1.50000E+02	8.23147E+01	3.94541E+01
5.00000E-01	1.75000E+02	8.02183E+01	3.84761E+01
5.00000E-01	2.00000E+02	7.72213E+01	3.70726E+01
5.00000E-01	3.00000E+02	6.27657E+01	3.02677E+01
5.00000E-01	4.00000E+02	4.99765E+01	2.42093E+01
5.00000E-01	5.00000E+02	4.03683E+01	1.96342E+01
5.00000E-01	7.00000E+02	2.77548E+01	1.35995E+01
5.00000E-01	1.00000E+03	1.77469E+01	8.79648E+00
5.00000E-01	2.00000E+03	7.38096E+00	3.86434E+00
5.00000E-01	3.00000E+03	4.28926E+00	2.45505E+00
5.00000E-01	4.00000E+03	2.82338E+00	1.82233E+00
5.00000E-01	5.00000E+03	2.01845E+00	1.53002E+00
5.00000E-01	7.00000E+03	1.20563E+00	1.34325E+00
5.00000E-01	1.00000E+04	7.07534E-01	1.35282E+00
5.00000E-01	2.00000E+04	2.63225E-01	1.94741E+00
5.00000E-01	3.00000E+04	1.48953E-01	2.74604E+00
5.00000E-01	4.00000E+04	1.00003E-01	3.65156E+00
5.00000E-01	5.00000E+04	7.66941E-02	4.58760E+00
5.00000E-01	7.00000E+04	5.90947E-02	6.59912E+00
5.00000E-01	9.50000E+04	5.39693E-02	8.84127E+00

Table 2

2 HDRL1C4N: Numerical Solution for Time-dep. T and P at R=0,Z=125

37 Number of lines to follow

1.25000E+02	2.50000E-01	5.25843E-01	8.21640E+01
1.25000E+02	5.00000E-01	1.04864E+00	1.63855E+02
1.25000E+02	1.00000E+00	2.08509E+00	3.25758E+02
1.25000E+02	2.00000E+00	4.12176E+00	6.43737E+02
1.25000E+02	3.00000E+00	6.11161E+00	9.54121E+02
1.25000E+02	4.00000E+00	8.05665E+00	1.25713E+03
1.25000E+02	5.00000E+00	9.95789E+00	1.55298E+03
1.25000E+02	7.00000E+00	1.36320E+01	2.12389E+03
1.25000E+02	1.00000E+01	1.88327E+01	2.93072E+03
1.25000E+02	2.00000E+01	3.37368E+01	5.23756E+03
1.25000E+02	3.00000E+01	4.54559E+01	7.05183E+03
1.25000E+02	4.00000E+01	5.45532E+01	8.47224E+03
1.25000E+02	5.00000E+01	6.14023E+01	9.56518E+03
1.25000E+02	7.00000E+01	7.00904E+01	1.10157E+04
1.25000E+02	1.00000E+02	7.48365E+01	1.19515E+04
1.25000E+02	1.10000E+02	7.50259E+01	1.20457E+04
1.25000E+02	1.25000E+02	7.44701E+01	1.20449E+04
1.25000E+02	1.50000E+02	7.21491E+01	1.17877E+04
1.25000E+02	1.75000E+02	6.89401E+01	1.13558E+04
1.25000E+02	2.00000E+02	6.53744E+01	1.08368E+04
1.25000E+02	3.00000E+02	5.19510E+01	8.70235E+03
1.25000E+02	4.00000E+02	4.16153E+01	6.96490E+03
1.25000E+02	5.00000E+02	3.41249E+01	5.68538E+03
1.25000E+02	7.00000E+02	2.41978E+01	3.99264E+03
1.25000E+02	1.00000E+03	1.59995E+01	2.61385E+03
1.25000E+02	2.00000E+03	6.94796E+00	1.12681E+03
1.25000E+02	3.00000E+03	4.10850E+00	6.68956E+02
1.25000E+02	4.00000E+03	2.73277E+00	4.48942E+02
1.25000E+02	5.00000E+03	1.96678E+00	3.27137E+02
1.25000E+02	7.00000E+03	1.18395E+00	2.03330E+02
1.25000E+02	1.00000E+04	6.98636E-01	1.27038E+02
1.25000E+02	2.00000E+04	2.61469E-01	5.91532E+01
1.25000E+02	3.00000E+04	1.48290E-01	4.22673E+01
1.25000E+02	4.00000E+04	9.97064E-02	3.55877E+01
1.25000E+02	5.00000E+04	7.65499E-02	3.29097E+01
1.25000E+02	7.00000E+04	5.90574E-02	3.21916E+01
1.25000E+02	9.50000E+04	5.39621E-02	3.36387E+01

Table 3

3 HDRL1C4N: Numerical Solution for Time-dep. T and P at R=0,Z=250

37 Number of lines to follow

2.50000E+02	2.50000E-01	2.59913E-01	1.61277E+02
2.50000E+02	5.00000E-01	5.16662E-01	3.20225E+02
2.50000E+02	1.00000E+00	1.02159E+00	6.31526E+02
2.50000E+02	2.00000E+00	2.00527E+00	1.23467E+03
2.50000E+02	3.00000E+00	2.95726E+00	1.81469E+03
2.50000E+02	4.00000E+00	3.87841E+00	2.37230E+03
2.50000E+02	5.00000E+00	4.77203E+00	2.91059E+03
2.50000E+02	7.00000E+00	6.48122E+00	3.93325E+03
2.50000E+02	1.00000E+01	8.86387E+00	5.34445E+03
2.50000E+02	2.00000E+01	1.54471E+01	9.14782E+03
2.50000E+02	3.00000E+01	2.03880E+01	1.18981E+04
2.50000E+02	4.00000E+01	2.40874E+01	1.38763E+04
2.50000E+02	5.00000E+01	2.68202E+01	1.52671E+04
2.50000E+02	7.00000E+01	3.02424E+01	1.68415E+04
2.50000E+02	1.00000E+02	3.22519E+01	1.74273E+04
2.50000E+02	1.10000E+02	3.24301E+01	1.73564E+04
2.50000E+02	1.25000E+02	3.24235E+01	1.71150E+04
2.50000E+02	1.50000E+02	3.19442E+01	1.65010E+04
2.50000E+02	1.75000E+02	3.11382E+01	1.57515E+04
2.50000E+02	2.00000E+02	3.01891E+01	1.49674E+04
2.50000E+02	3.00000E+02	2.63344E+01	1.21843E+04
2.50000E+02	4.00000E+02	2.30028E+01	1.00668E+04
2.50000E+02	5.00000E+02	2.02544E+01	8.49260E+03
2.50000E+02	7.00000E+02	1.59999E+01	6.30592E+03
2.50000E+02	1.00000E+03	1.17321E+01	4.37041E+03
2.50000E+02	2.00000E+03	5.80213E+00	2.02940E+03
2.50000E+02	3.00000E+03	3.61353E+00	1.24197E+03
2.50000E+02	4.00000E+03	2.47920E+00	8.48874E+02
2.50000E+02	5.00000E+03	1.82007E+00	6.25801E+02
2.50000E+02	7.00000E+03	1.12136E+00	3.94104E+02
2.50000E+02	1.00000E+04	6.72642E-01	2.48229E+02
2.50000E+02	2.00000E+04	2.56279E-01	1.15584E+02
2.50000E+02	3.00000E+04	1.46320E-01	8.15644E+01
2.50000E+02	4.00000E+04	9.88238E-02	6.74800E+01
2.50000E+02	5.00000E+04	7.61208E-02	6.12617E+01
2.50000E+02	7.00000E+04	5.89465E-02	5.78652E+01
2.50000E+02	9.50000E+04	5.39408E-02	5.85317E+01

Table 4

4 HDRL1C4N: Numerical Solution for Time-dep. T and P at R=0,Z=375

37 Number of lines to follow

3.75000E+02	2.50000E-01	1.26001E-05	7.32301E+01
3.75000E+02	5.00000E-01	2.78626E-05	1.46064E+02
3.75000E+02	1.00000E+00	8.03844E-05	2.90419E+02
3.75000E+02	2.00000E+00	2.94557E-04	5.73962E+02
3.75000E+02	3.00000E+00	5.68396E-04	8.50768E+02
3.75000E+02	4.00000E+00	7.65597E-04	1.12101E+03
3.75000E+02	5.00000E+00	9.04909E-04	1.38487E+03
3.75000E+02	7.00000E+00	1.22616E-03	1.89403E+03
3.75000E+02	1.00000E+01	2.51886E-03	2.61363E+03
3.75000E+02	2.00000E+01	1.65861E-02	4.67284E+03
3.75000E+02	3.00000E+01	5.27350E-02	6.29756E+03
3.75000E+02	4.00000E+01	1.31931E-01	7.57867E+03
3.75000E+02	5.00000E+01	2.85417E-01	8.58157E+03
3.75000E+02	7.00000E+01	7.66357E-01	9.97086E+03
3.75000E+02	1.00000E+02	1.79123E+00	1.10415E+04
3.75000E+02	1.10000E+02	2.17362E+00	1.12237E+04
3.75000E+02	1.25000E+02	2.75386E+00	1.13847E+04
3.75000E+02	1.50000E+02	3.67094E+00	1.14420E+04
3.75000E+02	1.75000E+02	4.50225E+00	1.13437E+04
3.75000E+02	2.00000E+02	5.23309E+00	1.11560E+04
3.75000E+02	3.00000E+02	7.14295E+00	1.01021E+04
3.75000E+02	4.00000E+02	8.00975E+00	9.02790E+03
3.75000E+02	5.00000E+02	8.27028E+00	8.08009E+03
3.75000E+02	7.00000E+02	8.01548E+00	6.54785E+03
3.75000E+02	1.00000E+03	7.01587E+00	4.94255E+03
3.75000E+02	2.00000E+03	4.31262E+00	2.57320E+03
3.75000E+02	3.00000E+03	2.92499E+00	1.65206E+03
3.75000E+02	4.00000E+03	2.11104E+00	1.16268E+03
3.75000E+02	5.00000E+03	1.60096E+00	8.73598E+02
3.75000E+02	7.00000E+03	1.02471E+00	5.62642E+02
3.75000E+02	1.00000E+04	6.31562E-01	3.60030E+02
3.75000E+02	2.00000E+04	2.47875E-01	1.70107E+02
3.75000E+02	3.00000E+04	1.43106E-01	1.20133E+02
3.75000E+02	4.00000E+04	9.73778E-02	9.90450E+01
3.75000E+02	5.00000E+04	7.54164E-02	8.94544E+01
3.75000E+02	7.00000E+04	5.87642E-02	8.34976E+01
3.75000E+02	9.50000E+04	5.39058E-02	8.34166E+01

Table 5

5 HDRL1C4N: Numerical Solution for T and P at R=0,T=50 Years

24 Number of lines to follow

5.00000E-01	5.00000E+01	6.24622E+01	3.00610E+01
1.00000E+01	5.00000E+01	6.24603E+01	7.70672E+02
2.00000E+01	5.00000E+01	6.24544E+01	1.54143E+03
3.00000E+01	5.00000E+01	6.24436E+01	2.31195E+03
5.00000E+01	5.00000E+01	6.24050E+01	3.85216E+03
7.00000E+01	5.00000E+01	6.23184E+01	5.38905E+03
9.75000E+01	5.00000E+01	6.20765E+01	7.49557E+03
1.25000E+02	5.00000E+01	6.14023E+01	9.56518E+03
1.52500E+02	5.00000E+01	5.98510E+01	1.15691E+04
1.80000E+02	5.00000E+01	5.62451E+01	1.33618E+04
2.05000E+02	5.00000E+01	4.98986E+01	1.46723E+04
2.30000E+02	5.00000E+01	3.91405E+01	1.53579E+04
2.50000E+02	5.00000E+01	2.68202E+01	1.52671E+04
2.70000E+02	5.00000E+01	1.53669E+01	1.45080E+04
2.90000E+02	5.00000E+01	8.21701E+00	1.33740E+04
3.10000E+02	5.00000E+01	4.09815E+00	1.21180E+04
3.42500E+02	5.00000E+01	1.18416E+00	1.01992E+04
3.75000E+02	5.00000E+01	2.85417E-01	8.58157E+03
4.37500E+02	5.00000E+01	1.42281E-02	6.34307E+03
5.00000E+02	5.00000E+01	1.04531E-02	4.87125E+03
5.62500E+02	5.00000E+01	6.52237E-04	3.86354E+03
6.25000E+02	5.00000E+01	3.60506E-04	3.14469E+03
6.87500E+02	5.00000E+01	3.01754E-05	2.61358E+03
7.50000E+02	5.00000E+01	1.08449E-05	2.21196E+03

Table 6

6 HDRL1C4N: Numerical Solution for T and P at R=0,T=100 Years

24 Number of lines to follow

5.00000E-01	1.00000E+02	8.07873E+01	3.87202E+01
1.00000E+01	1.00000E+02	8.07641E+01	9.93918E+02
2.00000E+01	1.00000E+02	8.06936E+01	1.98719E+03
3.00000E+01	1.00000E+02	8.05715E+01	2.97811E+03
5.00000E+01	1.00000E+02	8.01593E+01	4.95040E+03
7.00000E+01	1.00000E+02	7.94370E+01	6.89479E+03
9.75000E+01	1.00000E+02	7.77704E+01	9.50427E+03
1.25000E+02	1.00000E+02	7.48365E+01	1.19515E+04
1.52500E+02	1.00000E+02	7.01185E+01	1.41603E+04
1.80000E+02	1.00000E+02	6.29451E+01	1.59457E+04
2.05000E+02	1.00000E+02	5.39395E+01	1.70778E+04
2.30000E+02	1.00000E+02	4.26166E+01	1.75652E+04
2.50000E+02	1.00000E+02	3.22519E+01	1.74273E+04
2.70000E+02	1.00000E+02	2.26118E+01	1.68133E+04
2.90000E+02	1.00000E+02	1.51972E+01	1.58722E+04
3.10000E+02	1.00000E+02	9.80286E+00	1.47510E+04
3.42500E+02	1.00000E+02	4.43666E+00	1.28401E+04
3.75000E+02	1.00000E+02	1.79123E+00	1.10415E+04
4.37500E+02	1.00000E+02	2.71354E-01	8.30525E+03
5.00000E+02	1.00000E+02	4.95566E-02	6.39256E+03
5.62500E+02	1.00000E+02	7.83242E-03	5.07417E+03
6.25000E+02	1.00000E+02	1.60338E-03	4.13076E+03
6.87500E+02	1.00000E+02	2.31591E-04	3.43321E+03
7.50000E+02	1.00000E+02	6.25192E-05	2.90562E+03

Table 7

7 HDRL1C4N: Numerical Solution for T and P at R=0,T=500 Years

24 Number of lines to follow

5.00000E-01	5.00000E+02	4.03683E+01	1.96342E+01
1.00000E+01	5.00000E+02	4.03256E+01	5.01484E+02
2.00000E+01	5.00000E+02	4.01971E+01	1.00138E+03
3.00000E+01	5.00000E+02	3.99840E+01	1.49717E+03
5.00000E+01	5.00000E+02	3.93068E+01	2.47151E+03
7.00000E+01	5.00000E+02	3.83122E+01	3.40676E+03
9.75000E+01	5.00000E+02	3.64584E+01	4.61106E+03
1.25000E+02	5.00000E+02	3.41249E+01	5.68538E+03
1.52500E+02	5.00000E+02	3.13939E+01	6.61175E+03
1.80000E+02	5.00000E+02	2.83865E+01	7.36724E+03
2.05000E+02	5.00000E+02	2.55028E+01	7.90214E+03
2.30000E+02	5.00000E+02	2.25748E+01	8.28736E+03
2.50000E+02	5.00000E+02	2.02544E+01	8.49260E+03
2.70000E+02	5.00000E+02	1.79974E+01	8.60977E+03
2.90000E+02	5.00000E+02	1.58379E+01	8.64596E+03
3.10000E+02	5.00000E+02	1.38041E+01	8.60748E+03
3.42500E+02	5.00000E+02	1.08182E+01	8.41077E+03
3.75000E+02	5.00000E+02	8.27028E+00	8.08009E+03
4.37500E+02	5.00000E+02	4.61368E+00	7.21239E+03
5.00000E+02	5.00000E+02	2.35314E+00	6.22798E+03
5.62500E+02	5.00000E+02	1.11642E+00	5.28788E+03
6.25000E+02	5.00000E+02	4.89342E-01	4.46372E+03
6.87500E+02	5.00000E+02	2.03407E-01	3.78056E+03
7.50000E+02	5.00000E+02	7.95094E-02	3.22720E+03

Table 8

8 HDRL1C4N: Numerical Solution for T and P at R=0,T=1000 Years

24 Number of lines to follow

5.00000E-01	1.00000E+03	1.77469E+01	8.79648E+00
1.00000E+01	1.00000E+03	1.77352E+01	2.22224E+02
2.00000E+01	1.00000E+03	1.76999E+01	4.43950E+02
3.00000E+01	1.00000E+03	1.76413E+01	6.64538E+02
5.00000E+01	1.00000E+03	1.74547E+01	1.10094E+03
7.00000E+01	1.00000E+03	1.71792E+01	1.52645E+03
9.75000E+01	1.00000E+03	1.66614E+01	2.08869E+03
1.25000E+02	1.00000E+03	1.59995E+01	2.61385E+03
1.52500E+02	1.00000E+03	1.52098E+01	3.09618E+03
1.80000E+02	1.00000E+03	1.43164E+01	3.52726E+03
2.05000E+02	1.00000E+03	1.34325E+01	3.87223E+03
2.30000E+02	1.00000E+03	1.25005E+01	4.16849E+03
2.50000E+02	1.00000E+03	1.17321E+01	4.37041E+03
2.70000E+02	1.00000E+03	1.09535E+01	4.54050E+03
2.90000E+02	1.00000E+03	1.01734E+01	4.67947E+03
3.10000E+02	1.00000E+03	9.40005E+00	4.78744E+03
3.42500E+02	1.00000E+03	8.17584E+00	4.90102E+03
3.75000E+02	1.00000E+03	7.01587E+00	4.94255E+03
4.37500E+02	1.00000E+03	5.03385E+00	4.85287E+03
5.00000E+02	1.00000E+03	3.44077E+00	4.59525E+03
5.62500E+02	1.00000E+03	2.24429E+00	4.23541E+03
6.25000E+02	1.00000E+03	1.39700E+00	3.82895E+03
6.87500E+02	1.00000E+03	8.33468E-01	3.41890E+03
7.50000E+02	1.00000E+03	4.75818E-01	3.03192E+03

Table 9

9 HDRL1C4N: Numerical Solutions for Pathlines

100.	0.	1603.	24.
100.	125.	39400.	1102.
100.	250.	>100000.	923.
1000.	0.	2500.	13.
1000.	125.	3193.	326.
1000.	250.	6396.	643.
10000.	0.	>100000.	2.
10000.	125.	>100000.	135.
10000.	250.	>100000.	268.

List of SKB reports

Annual Reports

1977–78
TR 121
KBS Technical Reports 1 – 120.
Summaries. Stockholm, May 1979.

1979
TR 79–28
The KBS Annual Report 1979.
KBS Technical Reports 79-01 – 79-27.
Summaries. Stockholm, March 1980.

1980
TR 80–26
The KBS Annual Report 1980.
KBS Technical Reports 80-01 – 80-25.
Summaries. Stockholm, March 1981.

1981
TR 81–17
The KBS Annual Report 1981.
KBS Technical Reports 81-01 – 81-16.
Summaries. Stockholm, April 1982.

1982
TR 82–28
The KBS Annual Report 1982.
KBS Technical Reports 82-01 – 82-27.
Summaries. Stockholm, July 1983.

1983
TR 83–77
The KBS Annual Report 1983.
KBS Technical Reports 83-01 – 83-76
Summaries. Stockholm, June 1984.

1984
TR 85–01
Annual Research and Development Report 1984
Including Summaries of Technical Reports Issued during 1984. (Technical Reports 84-01– 84-19)
Stockholm June 1985.

1985
TR 85-20
Annual Research and Development Report 1985
Including Summaries of Technical Reports Issued during 1985. (Technical Reports 85-01-85-19)
Stockholm May 1986.

1986
TR86-31
SKB Annual Report 1986
Including Summaries of Technical Reports Issued during 1986
Stockholm, May 1987

Technical Reports

1987
TR 87-01
Radar measurements performed at the Klipperås study site
Seje Carlsten, Olle Olsson, Stefan Sehlstedt, Leif Stenberg
Swedish Geological Co, Uppsala/Luleå
February 1987

TR 87-02
Fuel rod D07/B15 from Ringhals 2 PWR: Source material for corrosion/leach tests in groundwater
Fuel rod/pellet characterization program part one
Roy Forsyth
Studsvik Energiteknik AB, Nyköping
March 1987